system, since GSH is mainly synthesized *de novo* in the liver, and hypothesize that the γ-glutamyl dipeptide levels may reflect hepatic dysfunction.

Drug-induced hepatotoxicity is a frequent cause of liver injury, and the predominant clinical presentation is acute hepatitis and/or cholestasis. Overdoses of APAP, the most commonly used analgesic and antipyretic, can lead to possibly fatal hepatitis and several hundred deaths attributable to this drug occur annually in the United States. Our DI samples were from patients with so-called idiosyncratic hepatotoxicity, and the underlying mechanisms of this disease remain unclear. Interestingly, the changes in the serum levels of γ-glutamyl dipeptides were similar among the DI samples although the causative drugs differed widely and the mechanisms responsible for the development of hepatotoxicity may also be different. Our findings revealed that the amount of γ-glutamyl dipeptide production attributable to a reduction in the hepatocellular GSH concentration was a common feature in drug-induced idiosyncratic hepatotoxicity. With AUC values of 0.817 (training data) and 0.849 (validation data) (Supplementary Table 3), the serum levels of ALT and γ-Glu-Citrulline could be used to distinguish between DI patients on the one hand and patients with viral hepatitis infection and healthy controls on the other (Table 2). Therefore, we suggest that these compounds represent noninvasive biomarkers that facilitate rapid screening for DI.

In summary, our CE–TOFMS and LC–MS/MS metabolomics-based analyses of serum samples from patients with liver diseases showed quantitative differences in γ-glutamyl dipeptides in various liver diseases. Our highly specific set of γ-glutamyl dipeptides, transaminases, and methionine sulfoxide enabled us to discriminate among liver diseases including DI, AHB, CHB, CNALT, CHC, CIR, and HCC, indicating that they can be used as multiple biomarkers in rapid screening for different types and stages of liver disease. Furthermore, we have shown that γ-glutamyl dipeptide synthesis was catalyzed by GCS, the enzyme that is feedback-inhibited by GSH, and thus the levels of these biomarkers were indicative of hepatic GSH production. As observed in patients with HCV-related liver diseases and NAFLD, the serum γ-glutamyl dipeptide levels tended to decrease during the course of liver disease progression, indicating an increase in oxidative stress resulting from decreased GSH production during liver disease progression. Therefore, γ-glutamyl dipeptide measurement can potentially provide valuable information about the hepatic reduction–oxidation state to gain insights into the role of oxidative stress in the pathogenesis and progression of liver diseases.

Conflict of interest

The Authors who have taken part in this study declared that they do not have anything to disclose regarding funding or conflict of interest with respect to this manuscript.

Financial support

This work was supported by Health and Labour Sciences Research Grants "Research on Biological Markers for New Drug Development" (T.S.) and "Research on Risk of Chemical Substances" (T.S.). Additional support was obtained through grants from the Ministry of Education, Culture, Sports, Science and Technology (MEXT) for a Global COE Program entitled "Human Metabolomic Systems Biology" in Life Sciences (T.S., M.T. and M.S.) and the ERATO Gas Biology Project (M.S.), as well as research funds from the Yamagata Prefectural Government and City of Tsuruoka.

Supplementary data

Supplementary data associated with this article can be found, in the online version, at doi:10.1016/j.jhep.2011.01.031.

References

[1] Loguercio C, Federico A. Oxidative stress in viral and alcoholic hepatitis. Free Radic Biol Med 2003;34:1–10.
[2] Brunt EM. Nonalcoholic steatohepatitis. Semin Liver Dis 2004;24:3–20.
[3] Younossi ZM, Jarrar M, Nugent C, Randhawa M, Afendy M, Stepanova M, et al. A novel diagnostic biomarker panel for obesity-related nonalcoholic steatohepatitis (NASH). Obes Surg 2008;18:1430–1437.
[4] Piccinino F, Sagnelli E, Pasquale G, Giusti G. Complications following percutaneous liver biopsy. A multicentre retrospective study on 68,276 biopsies. J Hepatol 1986;2:165–173.
[5] Bolukbas C, Bolukbas FF, Horoz M, Aslan M, Celik H, Erel O. Increased oxidative stress associated with the severity of the liver disease in various forms of hepatitis B virus infection. BMC Infect Dis 2005;5:95.
[6] Sreekumar A, Poisson LM, Rajendiran TM, Khan AP, Cao Q, Yu J, et al. Metabolomic profiles delineate potential role for sarcosine in prostate cancer progression. Nature 2009;457:910–914.
[7] Bogdanov M, Matson WR, Wang L, Matson T, Saunders-Pullman R, Bressman SS, et al. Metabolomic profiling to develop blood biomarkers for Parkinson's disease. Brain 2008;131:389–396.
[8] Wang C, Kong H, Guan Y, Yang J, Gu J, Yang S, et al. Plasma phospholipid metabolic profiling and biomarkers of type 2 diabetes mellitus based on high-performance liquid chromatography/electrospray mass spectrometry and multivariate statistical analysis. Anal Chem 2005;77:4108–4116.
[9] Sabatine MS, Liu E, Morrow DA, Heller E, McCarroll R, Wiegand R, et al. Metabolomic identification of novel biomarkers of myocardial ischemia. Circulation 2005;112:3868–3875.
[10] Kenny LC, Dunn WB, Ellis DI, Myers J, Baker PN, Consortium TG, et al. Novel biomarkers for pre-eclampsia detected using metabolomics and machine learning. Metabolomics 2005;1:227–234.
[11] Soga T, Ohashi Y, Ueno Y, Naraoka H, Tomita M, Nishioka T. Quantitative metabolome analysis using capillary electrophoresis mass spectrometry. J Proteome Res 2003;2:488–494.
[12] Soga T, Baran R, Suematsu M, Ueno Y, Ikeda S, Sakurakawa T, et al. Differential metabolomics reveals ophthalmic acid as an oxidative stress biomarker indicating hepatic glutathione consumption. J Biol Chem 2006;281:16768–16776.
[13] Soga T, Igarashi K, Ito C, Mizobuchi K, Zimmermann HP, Tomita M. Metabolomic profiling of anionic metabolites by capillary electrophoresis mass spectrometry. Anal Chem 2009;81:6165–6174.
[14] Shintani T, Iwabuchi T, Soga T, Kato Y, Yamamoto T, Takano N, et al. Cystathionine beta-synthase as a carbon monoxide-sensitive regulator of bile excretion. Hepatology 2009;49:141–150.
[15] Goto S, Okuno Y, Hattori M, Nishioka T, Kanehisa M. LIGAND: database of chemical compounds and reactions in biological pathways. Nucleic Acids Res 2002;30:402–404.
[16] Kaneto H, Xu G, Song KH, Suzuma K, Bonner-Weir S, Sharma A, et al. Activation of the hexosamine pathway leads to deterioration of pancreatic beta-cell function through the induction of oxidative stress. J Biol Chem 2001;276:31099–31104.
[17] Levine RL, Berlett BS, Moskovitz J, Mosoni L, Stadtman ER. Methionine residues may protect proteins from critical oxidative damage. Mech Ageing Dev 1999;107:323–332.
[18] Babior BM. Phagocytes and oxidative stress. Am J Med 2000;109:33–44.
[19] Vogt W. Oxidation of methionyl residues in proteins: tools, targets, and reversal. Free Radic Biol Med 1995;18:93–105.
[20] Griffith OW, Meister A. Potent and specific inhibition of glutathione synthesis by buthionine sulfoximine (*S-n*-butyl homocysteine sulfoximine). J Biol Chem 1979;254:7558–7560.
[21] Zalups RK, Lash LH. Depletion of glutathione in the kidney and the renal disposition of administered inorganic mercury. Drug Metab Dispos 1997;25:516–523.

[22] Ishizuka H, Konno K, Shiina T, Naganuma H, Nishimura K, Ito K, et al. Species differences in the transport activity for organic anions across the bile canalicular membrane. J Pharmacol Exp Ther 1999;290:1324–1330.
[23] Mainwaring GW, Williams SM, Foster JR, Tugwood J, Green T. The distribution of theta-class glutathione *S*-transferases in the liver and lung of mouse, rat and human. Biochem J 1996;318:297–303.
[24] Marrogi AJ, Khan MA, van Gijssel HE, Welsh JA, Rahim H, Demetris AJ, et al. Oxidative stress and p53 mutations in the carcinogenesis of iron overload-associated hepatocellular carcinoma. J Natl Cancer Inst 2001;93:1652–1655.
[25] Toyokuni S, Okamoto K, Yodoi J, Hiai H. Persistent oxidative stress in cancer. FEBS Lett 1995;358:1–3.
[26] Sutton A, Nahon P, Pessayre D, Rufat P, Poire A, Ziol M, et al. Genetic polymorphisms in antioxidant enzymes modulate hepatic iron accumulation and hepatocellular carcinoma development in patients with alcohol-induced cirrhosis. Cancer Res 2006;66:2844–2852.
[27] Koike K, Miyoshi H. Oxidative stress and hepatitis C viral infection. Hepatol Res 2006;34:65–73.
[28] Boya P, de la Pena A, Beloqui O, Larrea E, Conchillo M, Castelruiz Y, et al. Antioxidant status and glutathione metabolism in peripheral blood mononuclear cells from patients with chronic hepatitis C. J Hepatol 1999;31:808–814.
[29] Tanyalcin T, Taskiran D, Topalak O, Batur Y, Kutay F. The effects of chronic hepatitis C and B virus infections on liver reduced and oxidized glutathione concentrations. Hepatol Res 2000;18:104–109.
[30] Moriya K, Nakagawa K, Santa T, Shintani Y, Fujie H, Miyoshi H, et al. Oxidative stress in the absence of inflammation in a mouse model for hepatitis C virus-associated hepatocarcinogenesis. Cancer Res 2001;61:4365–4370.
[31] Sumida Y, Nakashima T, Yoh T, Nakajima Y, Ishikawa H, Mitsuyoshi H, et al. Serum thioredoxin levels as an indicator of oxidative stress in patients with hepatitis C virus infection. J Hepatol 2000;33:616–622.
[32] Bruix J. Treatment of hepatocellular carcinoma. Hepatology 1997;25:259–262.
[33] Szklaruk J, Silverman PM, Charnsangavej C. Imaging in the diagnosis, staging, treatment, and surveillance of hepatocellular carcinoma. Am J Roentgenol 2003;180:441–454.
[34] Kudo M, Takamine Y, Nakamura K, Shirane H, Uchida H, Kasakura S, et al. Des-gamma-carboxy prothrombin (PIVKA-II) and alpha-fetoprotein-producing IIc-type early gastric cancer. Am J Gastroenterol 1992;87:1859–1862.
[35] Takano S, Honda I, Watanabe S, Soda H, Nagata M, Hoshino I, et al. PIVKA-II-producing advanced gastric cancer. Int J Clin Oncol 2004;9:330–333.

JOURNAL OF VIROLOGY, Sept. 2011, p. 8556–8568 Vol. 85, No. 17
0022-538X/11/$12.00 doi:10.1128/JVI.00146-11

Hepatitis C Virus Infection Promotes Hepatic Gluconeogenesis through an NS5A-Mediated, FoxO1-Dependent Pathway▽

Lin Deng,[1] Ikuo Shoji,[1] Wataru Ogawa,[2] Shusaku Kaneda,[1] Tomoyoshi Soga,[3] Da-peng Jiang,[1] Yoshi-Hiro Ide,[1] and Hak Hotta[1]*

Division of Microbiology, Center for Infectious Diseases,[1] and Division of Diabetes, Metabolism and Endocrinology,[2] Kobe University Graduate School of Medicine, 7-5-1 Kusunoki-cho, Chuo-ku, Kobe 650-0017, Japan, and Institute for Advanced Biosciences, Keio University, 246-2 Mizukami, Kakuganji, Tsuruoka, Yamagata 997-0052, Japan[3]

Received 21 January 2011/Accepted 7 June 2011

Chronic hepatitis C virus (HCV) infection is often associated with type 2 diabetes. However, the precise mechanism underlying this association is still unclear. Here, using Huh-7.5 cells either harboring HCV-1b RNA replicons or infected with HCV-2a, we showed that HCV transcriptionally upregulated the genes for phosphoenolpyruvate carboxykinase (PEPCK) and glucose 6-phosphatase (G6Pase), the rate-limiting enzymes for hepatic gluconeogenesis. In this way, HCV enhanced the cellular production of glucose 6-phosphate (G6P) and glucose. PEPCK and G6Pase gene expressions are controlled by the transcription factor forkhead box O1 (FoxO1). We observed that although neither the mRNA levels nor the protein levels of FoxO1 expression were affected by HCV, the level of phosphorylation of FoxO1 at Ser319 was markedly diminished in HCV-infected cells compared to the control cells, resulting in an increased nuclear accumulation of FoxO1, which is essential for sustaining its transcriptional activity. It was unlikely that the decreased level of FoxO1 phosphorylation was mediated through Akt inactivation, as we observed an increased phosphorylation of Akt at Ser473 in HCV-infected cells compared to control cells. By using specific inhibitors of c-Jun N-terminal kinase (JNK) and reactive oxygen species (ROS), we demonstrated that HCV infection induced JNK activation via increased mitochondrial ROS production, resulting in decreased FoxO1 phosphorylation, FoxO1 nuclear accumulation, and, eventually, increased glucose production. We also found that HCV NS5A mediated increased ROS production and JNK activation, which is directly linked with the FoxO1-dependent increased gluconeogenesis. Taken together, these observations suggest that HCV promotes hepatic gluconeogenesis through an NS5A-mediated, FoxO1-dependent pathway.

Hepatitis C virus (HCV) is a small, enveloped RNA virus that belongs to the genus *Hepacivirus* of the family *Flaviviridae*, and the molecular mechanisms underlying its viral replication are currently being unraveled (40). The HCV genome encodes a single polyprotein of about 3,000 amino acids, which is cleaved by host and viral proteases to generate at least 10 viral proteins, such as core, envelope 1 (E1), E2, p7, NS2, NS3, NS4A, NS4B, NS5A, and NS5B. HCV can be classified into seven genotypes, with each genotype further classified into a number of subtypes, such as HCV-1a and HCV-1b (18, 24, 59).

HCV infects more than 120 million people worldwide (57). Persistent HCV infection causes not only liver diseases (chronic hepatitis, liver cirrhosis, and hepatocellular carcinoma) but also extrahepatic manifestations, such as type 2 diabetes (2, 11, 20, 23). While it is known that liver cirrhosis impairs the glucose metabolism of the liver, there are some reports showing that HCV-infected patients over 40 years of age have an increased risk of type 2 diabetes compared with individuals without HCV infection (43). In addition, insulin receptor substrate 1 (IRS-1)/phosphatidylinositol 3-kinase (PI3-kinase) signaling was more impaired in HCV-infected patients than in non-HCV-infected controls (3). These studies imply that HCV infection may directly predispose the host toward type 2 diabetes. However, the precise mechanisms are poorly understood.

Hepatocytes play an important role in maintaining plasma glucose homeostasis by adjusting the balance between hepatic glucose production and utilization via the gluconeogenic and glycolytic pathways, respectively. It was proposed previously that increased hepatic glucose production is a major feature of type 2 diabetes (13). It is also known that hyperglycemia and the subsequent development of type 2 diabetes mellitus result, at least in part, from impaired insulin signaling together with elevated glucagon levels (5, 19). Hepatic glucose production and utilization, physiologically opposed cascades, are regulated, at least in part, at the transcriptional level of the glucose 6-phosphatase (G6Pase) and glucokinase (GK) genes, which catalyze the last and the first rate-limiting steps in gluconeogenesis and glycolysis, respectively. A number of studies have shown that fasting/feeding (or hormones) controls the transcription of these two enzymes in the opposite directions. G6Pase transcription is negatively regulated by insulin or feeding and is markedly increased in a fasting state (62). On the other hand, GK transcription is positively regulated by insulin or feeding and markedly decreased in a fasting state (33). It has also been reported that the gene expressions of gluconeogenic and glycolytic enzymes, such as G6Pase, GK, and phosphoenolpyruvate carboxykinase (PEPCK), another rate-limiting enzyme for hepatic gluconeogenesis, are regulated by certain

* Corresponding author. Mailing address: Division of Microbiology, Center for Infectious Disease, Kobe University Graduate School of Medicine, 7-5-1 Kusunoki-cho, Chuo-ku, Kobe 650-0017, Japan. Phone: 81-78-382-5500. Fax: 81-78-382-5519. E-mail: hotta@kobe-u.ac.jp.

▽ Published ahead of print on 22 June 2011.

TABLE 1. Sequences and positions of primers used in this study

Gene (GenBank accession no.)	Primer	Positions	PCR product (bp)
GK (M69051)	5′-GCCTCCCAAAGCATCTACCTC-3′	119–139	444
	5′-GCTCCACTGCCCCTCCTCACC-3′	562–542	
G6Pase (U01120)	5′-CCTGGGGCTGGCTCTCAACTC-3′	889–909	309
	5′-AATAGTAGTCCTCCTCAATCC-3′	1197–1177	
PEPCK (BC023978)	5′-CCAGGCAGTGAGGGAGTTTCT-3′	210–230	217
	5′-ACTGTGTCTCTTTGCTCTTGG-3′	426–406	
FoxO1 (NM_002915)	5′-GAGGGTTAGTGAGCAGGTTAC-3′	2352–2372	217
	5′-AGTCCTTATCTACAGCAGCAC-3′	2568–2548	
HCV NS5A (JF343793)	5′-AGACGTATTGAGGTCCATGC-3′	6899–6918	133
	5′-CCGCAGCGACGGTGCTGATAG-3′	7011–7031	
β-Glucuronidase (M15182)	5′-ATCAAAAACGCAGAAAATACG-3′	1747–1767	238
	5′-ACGCAGGTGGTATCAGTCTTG-3′	1984–1964	
GAPDH (NM_002046)	5′-GCCATCAATGACCCCTTCATT-3′	196–216	149
	5′-TCTCGCTCCTGGAAGATGG-3′	326–344	

transcription factors, including forkhead box O1 (FoxO1) (26, 50, 54), hepatic nuclear factor 4α (HNF-4α) (26), Krüppel-like factor 15 (KLF15) (64), and cyclic AMP (cAMP) response element binding protein (CREB) (52, 56). The deregulation of the otherwise balanced control of hepatic glucose homeostasis would potentially lead to hyperglycemia and, eventually, type 2 diabetes.

In this study, by using Huh-7.5 cells harboring HCV-1b RNA replicons, i.e., either a subgenomic RNA replicon (SGR) or a full-genomic RNA replicon (FGR) (37), and cells infected with HCV-2a (14, 37, 39), we investigated the possible effects of HCV on glucose metabolism. We report here that HCV promotes hepatic gluconeogenesis, resulting in increased cellular glucose production in hepatocytes via an NS5A-mediated, FoxO1-dependent pathway.

MATERIALS AND METHODS

Cells, HCV RNA replicons, and virus. The human hepatoma-derived cell line Huh-7.5 (7) was kindly provided by C. M. Rice (Rockefeller University, New York, NY). The SGR and FGR were prepared by using pFK5B/2884Gly (41) (a kind gift from R. Bartenschlager, University of Heidelberg, Heidelberg, Germany) and pON/C-5B (31) (a kind gift from N. Kato, Okayama University, Okayama, Japan), respectively. The SGR and FGR cells are of polyclonal origin to avoid clonal variation. Plasmid pFL-J6/JFH1, which encodes the entire viral genome of a chimeric strain of HCV-2a (J6/JFH1) (39), was kindly provided by C. M. Rice. The HCV RNA genome was transcribed *in vitro* from pFL-J6/JFH1 and transfected into Huh-7.5 cells to yield infectious HCV particles, as described previously (14). A cell culture-adapted P-47 strain (9, 14) was used throughout the experiments. Virus infection was performed at a multiplicity of infection (MOI) of 2.0. Virus infectivity was measured by indirect immunofluorescence analysis, as described below, and expressed as cell-infecting units/ml. In some experiments, SGR and FGR cells, as well as HCV-infected cells at 5 days after virus infection, were treated with 1,000 IU/ml of alpha interferon (IFN) (Sigma Chemical, St. Louis, MO) for 10 days to eliminate HCV replication.

Plasmid construction. Expression plasmids for core, p7, NS2, NS3, NS3/4A, NS4A, NS4B, NS5A, and NS5B were reported elsewhere previously (15, 32).

Real-time quantitative RT-PCR. Total cellular RNA was isolated by using RNAiso reagent (Takara, Kyoto, Japan), and cDNA was generated by using a QuantiTect reverse transcription (RT) system (Qiagen, Valencia, CA). Real-time quantitative PCR was performed by using SYBR Premix Ex *Taq* (Takara) with SYBR green chemistry on an ABI Prism 7000 system (Applied Biosystems, Foster City, CA), as reported previously (37). β-Glucuronidase and GAPDH (glyceraldehyde-3-phosphate dehydrogenase) were used as internal controls. The primers used are shown in Table 1.

G6P production assay. Huh-7.5 cells seeded into a 10-cm dish at a density of 1.0×10^6 cells/dish were infected with HCV or left uninfected. At different time points after infection, the cells were washed twice with 5% mannitol solution and covered with methanol (1 ml) containing 25 μM (each) four internal standards (3-aminopyrolidine, L-methionine sulfone, trimesate, and 2-morpholinoethanesulfonic acid) for enzyme inactivation. The mixtures of methanol and cells were collected and mixed with Milli-Q water and chloroform at ratios of 2:1:2. Both the medium and cell sample solutions were then centrifuged at 20,000 × *g* for 15 min, and the aqueous layers were collected for centrifugal filtration through a 5-kDa-cutoff filter at 9,000 × *g* for 2 h. The extracted metabolites were concentrated with a centrifugal concentrator and stored at −80°C until analysis. Glucose 6-phosphate (G6P) concentrations were measured by capillary electrophoresis time-of-flight mass spectrometry (CE-TOFMS), and the results were normalized to the cell number as described previously (60, 61).

Glucose production assay. Culture medium was replaced with glucose production buffer consisting of glucose-free Dulbecco's modified Eagle's medium (DMEM) (Sigma Chemical), without phenol red, supplemented with a gluconeogenic substrate (2 mM sodium pyruvate and 20 mM sodium lactate). After 24 h of incubation, the medium was collected, and the total glucose concentration was measured by using a commercial kit (Glucose CII Test Wako; Wako Pure Chemical Industries, Osaka, Japan) and normalized to the cellular protein content. As the baseline of glucose production, glucose-free DMEM with neither sodium pyruvate nor sodium lactate was used. Glucose production via gluconeogenesis equals the total glucose production minus the baseline glucose production.

Luciferase reporter assay. The PEPCK gene promoter (position −1263/+225) and a deletion mutant (position −998/+225) were inserted into the pGL3 luciferase reporter plasmid (Promega, Madison, WI). The constructs were designated rPEPCK-P5(−1263)-pGL3basic and rPEPCK-P4(−998)-pGL3basic. pRL-CMV-Renilla (Promega), which expresses *Renilla* luciferase, was used as an internal control. Huh-7.5 cells prepared in a 12-well tissue culture plate at a density of 1.0×10^5 cells/well were transiently transfected with pRL-CMV-Renilla and rPEPCK-P5(−1263)-pGL3basic or rPEPCK-P4(−998)-pGL3basic in the presence of pEF1/NS4A, pEF1/NS5A, or a control vector (32). After 48 h, a luciferase assay was performed by using the Dual-Luciferase reporter assay system (Promega). Firefly and *Renilla* luciferase activities were measured with a Lumat LB 9501 luminometer (Berthold, Bad Wildbad, Germany). Firefly luciferase activity was normalized to *Renilla* luciferase activity for each sample.

Detection of mitochondrial ROS. Mitochondrial reactive oxygen species (ROS) production was analyzed as described previously (14). Briefly, cells seeded onto glass coverslips in a 24-well plate were incubated with 5 μM MitoSOX red (Molecular Probes, Eugene, OR) at 37°C for 10 min and then fixed with 3.7% paraformaldehyde and observed under a confocal laser scanning microscope (Carl Zeiss, Oberkochen, Germany). When needed, the fixed cells

were subjected to indirect immunofluorescence analysis to confirm HCV infection or NS5A expression, as described below.

Indirect immunofluorescence. Huh-7.5 cells seeded onto glass coverslips in a 24-well plate were infected with HCV or transfected with an NS5A expression plasmid. At 5 days postinfection (dpi) or 3 days posttransfection, the cells were fixed with 3.7% paraformaldehyde in phosphate-buffered saline (PBS) for 15 min at room temperature and permeabilized with 0.1% Triton X-100 in PBS for 15 min at room temperature. Mock-infected or empty-vector-transfected cells were similarly treated as controls for comparisons. After being washed with PBS twice, cells were consecutively stained with primary and secondary antibodies. The primary antibodies used were anti-FoxO1 rabbit monoclonal antibody (Cell Signaling Technology, Danvers, MA), anti-NS5A mouse monoclonal antibody (Chemicon International, Temecula, CA), and serum from an HCV-infected patient. Secondary antibodies used were Alexa Fluor 488-conjugated goat anti-rabbit immunoglobulin G (IgG), Alexa Fluor 594-conjugated goat anti-mouse IgG or anti-human IgG (Molecular Probes), and fluorescein isothiocyanate (FITC)-conjugated goat anti-mouse IgG or anti-human IgG (MBL, Nagoya, Japan). The stained cells were observed under a confocal laser scanning microscope (Carl Zeiss).

Cell fractionation and immunoblotting. Nuclear and cytoplasmic extracts from cells were prepared by using an NE-PER nuclear and cytoplasmic extraction reagent kit (Pierce Chemical, Rockford, IL). For immunoblotting, cells were lysed with SDS sample buffer, and equal amounts of protein were subjected to SDS-polyacrylamide gel electrophoresis and transferred onto a polyvinylidene difluoride membrane (Millipore, Bedford, MA), which was then incubated with the respective primary antibodies. The primary antibodies used were mouse monoclonal antibodies against HCV core (clone 2H9; a kind gift from T. Wakita, Department of Virology II, National Institute of Infectious Diseases, Tokyo, Japan), NS3, NS4A, NS5A, GAPDH (Chemicon), FoxO1 (Sigma Chemical), phospho-Akt (Ser473) (Cell Signaling Technology), and c-Myc (9E10; Santa Cruz Biotechnology, Santa Cruz, CA); rabbit polyclonal antibodies against phospho-FoxO1 (Ser139), Oct-1 (Santa Cruz Biotechnology), c-Jun N-terminal kinase (JNK), phospho-JNK (Thr183/Tyr185), c-Jun, phospho-c-Jun (Ser63), and Akt (Cell Signaling Technology); and goat polyclonal antibody against HSP60 (Santa Cruz Biotechnology). Horseradish peroxidase-conjugated goat anti-mouse IgG, goat anti-rabbit IgG (Molecular Probes), and donkey anti-goat IgG (Santa Cruz Biotechnology) were used to visualize the respective proteins by means of an enhanced chemiluminescence detection system (ECL; GE Healthcare, Buckinghamshire, United Kingdom).

Statistical analysis. Results were expressed as means ± standard errors of the means (SEM). Statistical significance was evaluated by analysis of variance (ANOVA) and was defined as a P value of <0.05.

RESULTS

HCV upregulates gene expression of PEPCK and G6Pase and downregulates gene expression of GK. We first examined the expression levels of the genes for the rate-limiting enzymes in hepatic gluconeogenesis, PEPCK and G6Pase, and of those for GK, which catalyzes the first step of glycolysis, by means of real-time quantitative RT-PCR analysis. We observed that the PEPCK and G6Pase genes were transcriptionally activated in SGR- and FGR-harboring cells (Fig. 1A and B, left). Similarly, the PEPCK and G6Pase genes were upregulated in HCV-infected cells in a time-dependent manner, starting from 3 or 5 days postinfection (dpi) up to 14 dpi (Fig. 1A and B, middle). On the other hand, the GK gene was transcriptionally downregulated in SGR- and FGR-harboring cells and HCV-infected cells in a time-dependent manner (Fig. 1C). It is noteworthy that the gene expressions of six glycolytic enzymes (not including GK) were observed to be upregulated in HCV-infected cells at 1 dpi (16).

When IFN treatment eliminated HCV from the cells, the observed upregulation of PEPCK and G6Pase gene expressions as well as the downregulation of GK gene expression in SGR- and FGR-harboring cells and HCV-infected cells were cancelled (Fig. 1A, B, and C, left and right). Thus, our results suggest that there was a trend toward an increase in gluconeogenesis in SGR- and FGR-harboring cells and HCV-infected cells. In subsequent studies we further examined whether or not HCV replication was correlated with gluconeogenesis.

HCV promotes cellular production of glucose and G6P. We then examined the effect of HCV on cellular glucose production. The results showed that SGR- and FGR-harboring cells and HCV-infected cells produced greater amounts of glucose than did the control cells (Fig. 2A, top and middle). IFN treatment cancelled the enhanced glucose production in SGR- and FGR-harboring cells and in HCV-infected cells (Fig. 2A, top and bottom). We also investigated the production of G6P, which is an important precursor molecule that is converted to glucose in the gluconeogenesis pathway, by means of metabolome analysis. As shown in Fig. 2B, a significantly higher level of G6P was accumulated in HCV-infected cells than in control cells. Taken together, these results indicate that HCV indeed promotes hepatic gluconeogenesis to cause hyperglycemia. In the following analyses, we examined the possible mechanisms of HCV-induced increased gluconeogenesis.

HCV suppresses FoxO1 phosphorylation at Ser319, leading to the nuclear accumulation of FoxO1. It was demonstrated previously that FoxO1 in hepatocytes enhances gluconeogenesis through the transcriptional activation of various genes, including G6Pase and PEPCK (25). To investigate the possible effects of FoxO1 on HCV-induced gluconeogenesis, we examined the gene expression levels of FoxO1 by real-time quantitative RT-PCR analysis. As shown in Fig. 3A, there was neither an upregulation nor a downregulation of FoxO1 gene expression in SGR- or FGR-harboring cells or HCV-infected cells. The FoxO1 transcription factor is controlled by various post-translational modifications, which include phosphorylation, ubiquitylation, and acetylation. The phosphorylated form of FoxO1 is exported from the nucleus and thereby loses its transcriptional function (30). We therefore examined the phosphorylation status of FoxO1 at Ser319, which is critical for FoxO1 nuclear exclusion (72). The results showed that FoxO1 phosphorylation at Ser319 was markedly suppressed in HCV-infected cells from 4 dpi up to 8 dpi, compared to that in the HCV-negative control cells (Fig. 3B, first panel), in a time-dependent manner that was roughly the inverse of the pattern observed for PEPCK and G6Pase mRNA upregulations (Fig. 1A and B) and glucose production (Fig. 2A), while the total protein expression levels of FoxO1 were unchanged (Fig. 3B, second panel). Regarding this connection, Banerjee et al. reported previously that FoxO1 phosphorylation at Ser256 was also inhibited in HCV-infected cells (4). Since FoxO1 is known to be phosphorylated by Akt so as to be exported from the nucleus and transcriptionally inactivated (38), we examined whether Akt function was suppressed through its impaired phosphorylation in HCV-infected cells. The result obtained revealed that this was not the case: Akt phosphorylation was enhanced in HCV-infected cells from 4 dpi up to 6 dpi compared with the control cells (Fig. 3B, third panel), while the total protein expression levels of Akt were comparable (Fig. 3B, fourth panel). This result is consistent with a recent observation by Burdette et al. (10) showing that the Akt phosphorylation level was elevated in HCV-infected cells. These data suggest that the observed decrease in FoxO1 phosphorylation

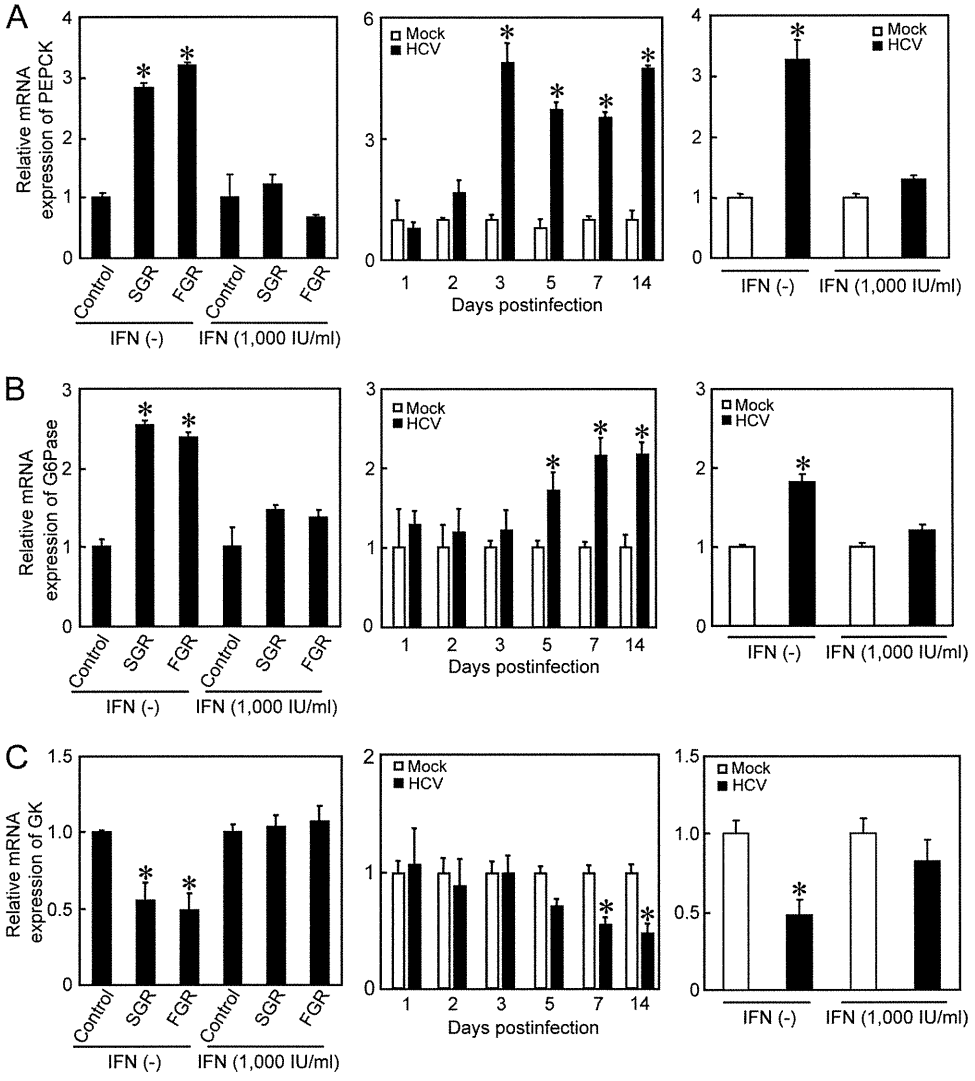

FIG. 1. HCV upregulates gene expressions of PEPCK and G6Pase and downregulates gene expression of GK. Quantitative RT-PCR analysis was performed to quantify PEPCK (A), G6Pase (B), and GK (C) mRNA expression levels in SGR- and FGR-harboring cells and HCV-infected cells (MOI = 2), and the results were normalized to β-glucuronidase mRNA expression levels. In parallel, SGR- and FGR-harboring cells and HCV-infected cells (at 5 dpi) were treated with IFN (1,000 IU/ml) for 10 days to eliminate HCV replication before being subjected to quantitative RT-PCR. Data represent means ± SEM of data from three independent experiments, and the values for the control cells were arbitrarily expressed as 1.0. *, $P < 0.01$ compared with the control.

in HCV-infected cells is caused by a mechanism independent of Akt.

Next, we tested whether HCV indeed promoted FoxO1 nuclear accumulation. The majority of FoxO1 was accumulated in the nuclear fraction in HCV-infected cells (Fig. 3C, second panel, lanes 2 and 4), whereas in control cells FoxO1 was distributed in both the nuclear and cytoplasmic fractions (lanes 1 and 3). Taken together, these results suggest that HCV suppressed FoxO1 phosphorylation, leading to the nuclear accumulation of FoxO1.

HCV-induced JNK activation is involved in the suppression of FoxO1 phosphorylation. Recent studies demonstrated that a signaling pathway that involves the stress-sensitive serine/threonine kinase JNK regulates FoxO at multiple levels (36, 66). We therefore investigated whether HCV induced JNK activation in Huh-7.5 cells. As shown in Fig. 4A, the amount of phosphorylated (activated) JNK markedly increased in HCV-infected cells in a time-dependent manner, similar to that observed for the suppression of FoxO1 phosphorylation, while the total expression levels of JNK were unchanged. As a result, c-Jun, a key substrate for JNK, was phosphorylated (activated) in HCV-infected cells but not in the mock-infected control cells. It should also be noted that the total expression levels of c-Jun in HCV-infected cells were significantly higher than those in the mock-infected control cells, suggesting that c-Jun activation through its phosphorylation stabilizes c-Jun protein expression in HCV-infected cells, as was proposed previously by Zhang et al (71).

We next sought to determine whether JNK activation was involved in the HCV-induced suppression of FoxO1 phosphorylation. HCV-infected cells at 5 days after virus infection were treated with the specific JNK inhibitor SP600125 (20 μM) (6)

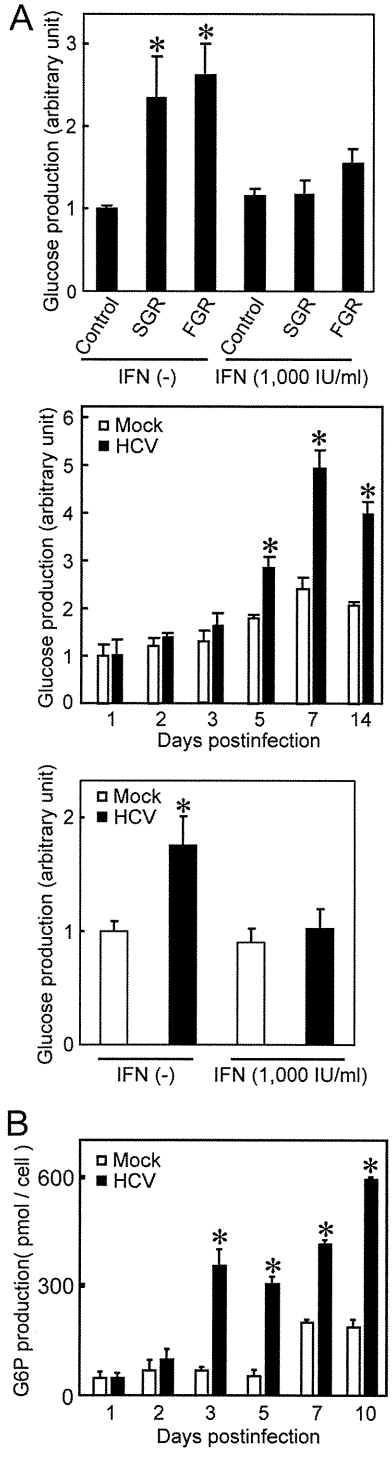

FIG. 2. HCV promotes the production of glucose and G6P. (A) Extracellular glucose production was measured in SGR- and FGR-harboring cells and HCV-infected cells (MOI = 2) and normalized to total cellular protein expression levels. In parallel, SGR- and FGR-harboring cells and HCV-infected cells (at 5 dpi) were treated with IFN (1,000 IU/ml) for 10 days to eliminate HCV replication before being subjected to glucose production analysis. Data represent means ± SEM of data from three independent experiments, and the value for the control cells was arbitrarily expressed as 1.0. *, $P < 0.01$ compared with the control. (B) Cellular G6Pase production was measured in HCV-infected cells (MOI = 2), and the results were normalized to cell numbers. Data represent means ± SEM of data from three independent experiments. *, $P < 0.01$ compared with the control.

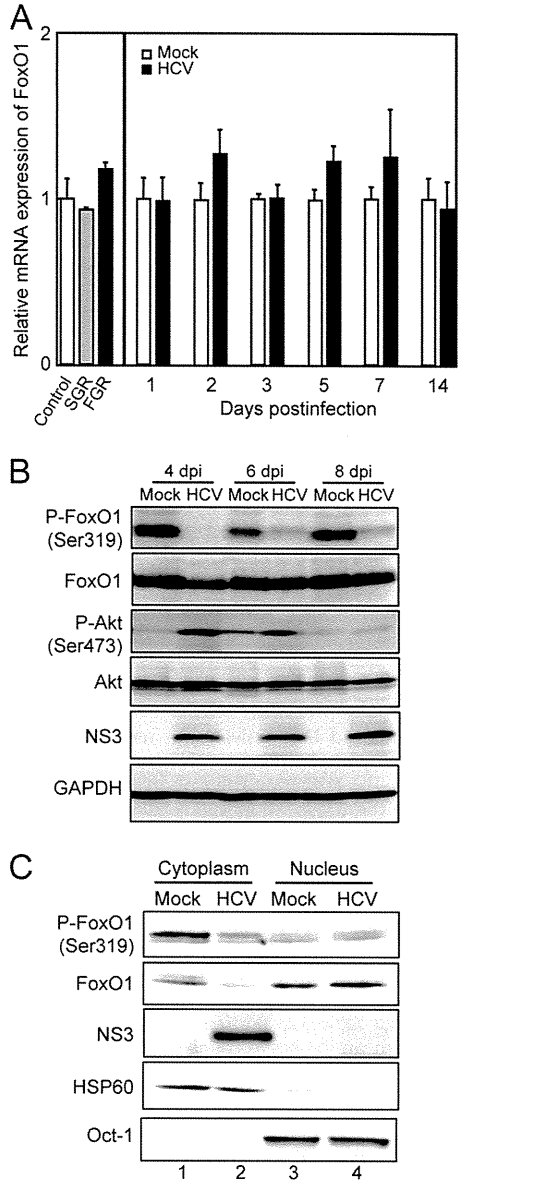

FIG. 3. HCV suppresses FoxO1 phosphorylation, leading to nuclear accumulation of FoxO1. (A) Quantitative RT-PCR analysis was performed to determine FoxO1 mRNA expression levels in SGR- and FGR-harboring cells and HCV-infected cells (MOI = 2), and expression levels were normalized to β-glucuronidase mRNA expression levels. (B) The expression levels of FoxO1, phospho-FoxO1 (Ser319) (P-FoxO1), Akt, and phospho-Akt (Ser473) were analyzed by immunoblotting of HCV-infected cells and mock-infected control cells. Blots were reprobed with antibodies recognizing NS3 and GAPDH. The amounts of GAPDH were measured as an internal control to verify equal amounts of sample loading. (C) Cytoplasmic and nuclear fractions were prepared from HCV-infected cells and mock-infected control cells at 4 dpi and were analyzed by immunoblotting using antibodies against FoxO1, phospho-FoxO1 (Ser319), NS3, Hsp60, and Oct-1. The amounts of Hsp60 and Oct-1 were measured to verify that they were equal to the amounts of cytoplasmic and nuclear fractions, respectively.

for 24 h. The catalytic JNK activity was assayed by monitoring the phosphorylation of c-Jun. As shown in Fig. 4B, SP600125 clearly prevented the phosphorylation of c-Jun and concomitantly recovered the suppression of FoxO1 phosphorylation in

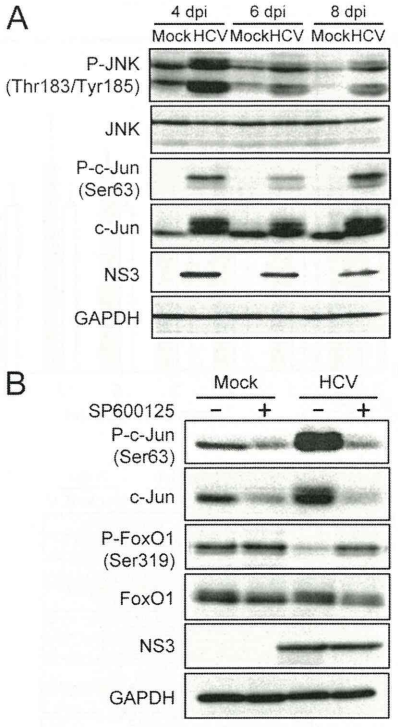

FIG. 4. HCV-induced JNK activation is required for the suppression of FoxO1 phosphorylation. (A) HCV activates the JNK/c-Jun signaling pathway. The activation (phosphorylation) of JNK (Thr183/Tyr185) and c-Jun (Ser63) in whole-cell lysates of HCV-infected cells and mock-infected control cells was analyzed by immunoblotting. Blots were reprobed with antibodies recognizing total JNK and c-Jun, NS3, and GAPDH. The amounts of GAPDH were measured as an internal control to verify equal amounts of sample loading. (B) Pretreatment with the JNK inhibitor SP600125 abrogates HCV-induced c-Jun activation and FoxO1 phosphorylation suppression. The phosphorylation of c-Jun (Ser63) and that of FoxO1 (Ser319) were analyzed by immunoblotting at 6 dpi in HCV-infected cells and mock-infected control cells with or without SP600125 pretreatment (20 μM for 24 h). Blots were reprobed with antibodies recognizing total c-Jun and FoxO1, NS3, and GAPDH. The amounts of GAPDH were measured as an internal control to verify equal amounts of sample loading.

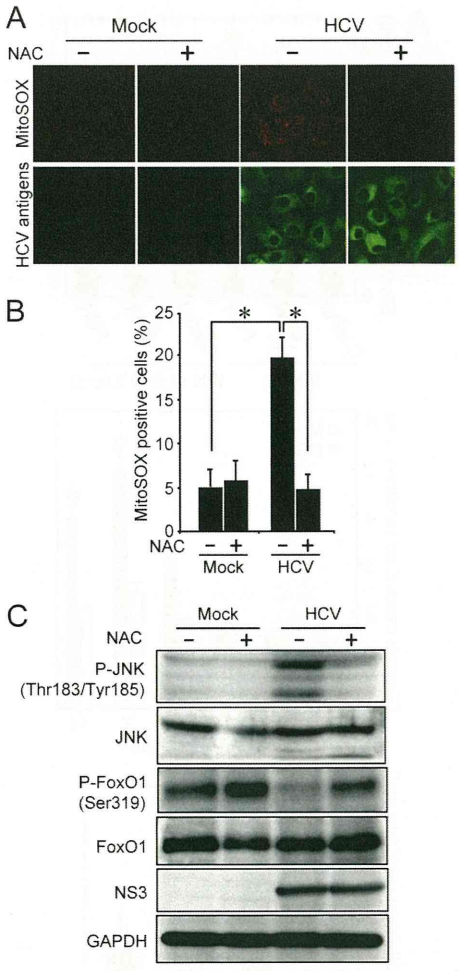

FIG. 5. HCV-induced production of mitochondrial ROS suppresses FoxO1 phosphorylation through activation of JNK. (A) Pretreatment with NAC abrogates the HCV-induced increased production of mitochondrial ROS. HCV-infected cells and mock-infected controls were pretreated with 5 mM NAC for 2 h at 6 dpi. The cells were then incubated with MitoSOX (top) and then stained for HCV antigens by using serum from an HCV-infected patient, followed by FITC-conjugated goat anti-human IgG (bottom). (B) Quantification of MitoSOX-stained cells. The percentages of cells stained with MitoSOX were determined for HCV-infected cells and mock-infected controls with or without NAC pretreatment. Data represent means ± SEM of data from two independent experiments. *, $P < 0.01$. (C) NAC pretreatment abrogates HCV-induced JNK activation and FoxO1 phosphorylation suppression. The phosphorylation of JNK (Thr183/Tyr185) and that of FoxO1 (Ser319) were analyzed by immunoblotting at 6 dpi in HCV-infected cells and mock-infected controls with or without NAC pretreatment (5 mM for 2 h). The blots were reprobed with antibodies recognizing total JNK and FoxO1, NS3, and GAPDH. The amounts of GAPDH were measured as an internal control to verify equal amounts of sample loading.

HCV-infected cells. These results suggest that HCV activates the JNK/c-Jun signaling pathway, which induces the nuclear accumulation of FoxO1 by reducing its phosphorylation status.

HCV-induced mitochondrial ROS production is involved in FoxO1 phosphorylation suppression, FoxO1 nuclear accumulation, and increased glucose production through JNK activation. We previously reported that HCV infection increases mitochondrial ROS production (14). JNK is known to be activated by ROS (35). We therefore sought to determine whether the HCV-induced increase in ROS production is an event occurring upstream of JNK activation by HCV. The pretreatment of HCV-infected cells (at 6 dpi) with 5 mM *N*-acetyl cysteine (NAC) (a general antioxidant) for 2 h significantly reduced the HCV-induced increase in ROS levels (Fig. 5A and B), as revealed by using MitoSOX, a fluorescent probe specific for superoxide that selectively accumulates in the mitochondrial compartment. As shown in Fig. 5C, NAC clearly prevented the phosphorylation of JNK and concomitantly recovered the suppression of FoxO1 phosphorylation in HCV-infected cells. These results suggest that HCV-induced ROS production is involved in JNK activation, which results in the inhibition of FoxO1 phosphorylation.

We next investigated the effects of JNK activation and ROS production on the subcellular localization of FoxO1 in HCV-infected cells by indirect immunofluorescence staining. As shown in Fig. 6A and B, FoxO1 was localized predominantly in the cytoplasm of mock-infected control cells. On the other

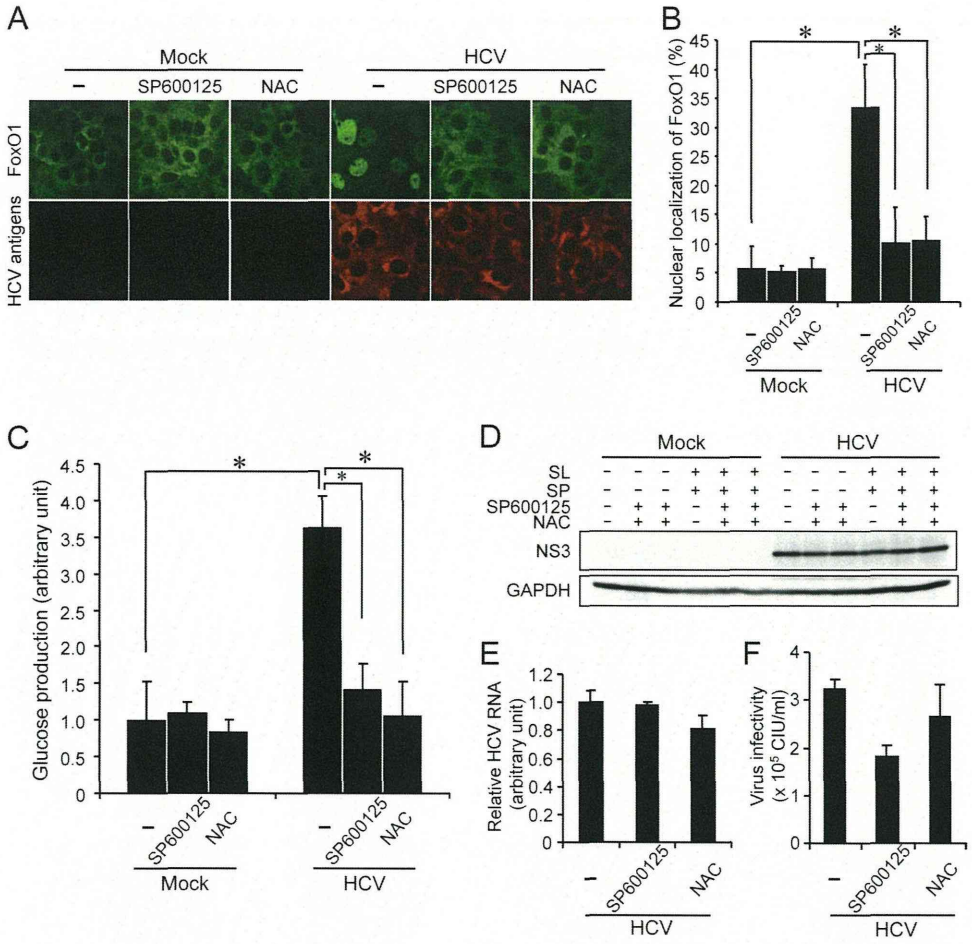

FIG. 6. HCV-induced JNK activation and ROS production are involved in FoxO1 nuclear accumulation and increased glucose production. (A) Subcellular localization of FoxO1 in HCV-infected cells and mock-infected controls with or without JNK inhibitor (SP600125 at 20 μM for 24 h) or antioxidant (NAC at 5 mM for 2 h) pretreatment at 5 dpi was examined by confocal microscopy. After fixation and permeabilization, the cells were incubated with an anti-FoxO1 rabbit monoclonal antibody followed by Alexa Fluor 488-conjugated goat anti-rabbit IgG (top) and with serum from an HCV-infected patient followed by Alexa Fluor 594-conjugated goat anti-human IgG (bottom). (B) The percentages of cells with FoxO1 nuclear localization were determined for HCV-infected cells and mock-infected controls with or without SP600125 or NAC pretreatment. Data represent means ± SEM of data from two independent experiments. *, $P < 0.01$. (C) Extracellular glucose production was measured in HCV-infected cells and mock-infected controls with or without SP600125 or NAC pretreatment at 7 dpi and normalized to total cellular protein expression levels. Data represent means ± SEM of data from two independent experiments, and the value for the control cells was arbitrarily expressed as 1.0. *, $P < 0.01$. (D) Cellular expression levels of NS3 in HCV-infected cells and mock-infected control cells with or without sodium lactate (SL), sodium pyruvate (SP), SP600125, or NAC are shown. The amounts of GAPDH were measured as an internal control to verify equal amounts of sample loading. (E) Amounts of HCV RNA were measured by quantitative RT-PCR analysis of HCV-infected cells treated with SP600125 or NAC or left untreated at 6 dpi. The amounts were normalized to GAPDH mRNA expression levels. Data represent means ± SEM of data from two independent experiments, and the value for the nontreated HCV-infected cells was arbitrarily expressed as 1.0. (F) Virus infectivity in the culture supernatants of HCV-infected cells treated with SP600125 or NAC or left untreated at 6 dpi was measured. Data represent means ± SEM of data from two independent experiments. CIU, cell-infecting units.

hand, the nuclear accumulation of FoxO1 was clearly observed in approximately 35% of HCV-infected cells at 5 dpi. The treatment of HCV-infected cells with a JNK inhibitor (SP600125 at 20 μM for 24 h) or an antioxidant (NAC at 5 mM for 2 h) significantly inhibited HCV-induced FoxO1 nuclear accumulation.

To further verify the role played by JNK activation and ROS production in HCV-induced hepatic gluconeogenesis, the glucose production in SP600125- or NAC-treated HCV-infected cells was assessed. Treatment with SP600125 or NAC significantly impaired the HCV-induced increased glucose production at 7 dpi (Fig. 6C) but did not affect the overall abundance of the HCV NS3 protein (Fig. 6D). We also examined the possible effects of SP600125 or NAC on HCV RNA replication and infectious-virus production. The results obtained revealed that treatment with SP600125 (20 μM for 24 h) or NAC (5 mM for 2 h) barely affected HCV RNA replication (Fig. 6E). On the other hand, we noted a tendency for infectious-virus production to be only slightly suppressed by SP600125 but not by NAC (Fig. 6F). A short-term inhibition of glucose production might not sufficiently affect HCV RNA replication or virus production.

Taken together, these results indicate that ROS-mediated JNK activation plays a key role in the suppression of FoxO1

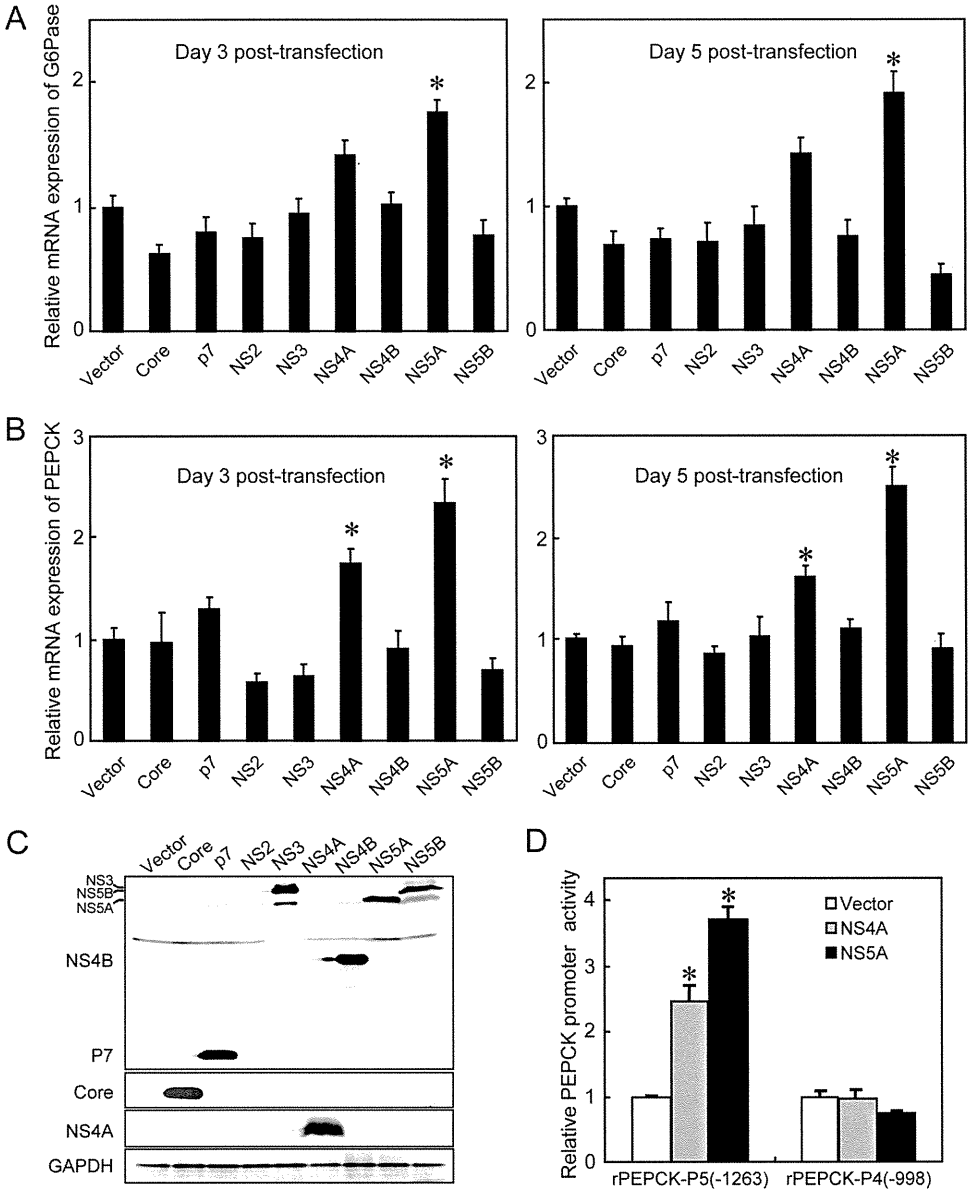

FIG. 7. HCV NS5A is involved in increased mRNA expression levels for G6Pase and PEPCK. Huh-7.5 cells were transfected with the indicated HCV viral protein expression plasmids. (A and B) At 3 and 5 days posttransfection, quantitative RT-PCR analyses of mRNA for G6Pase (A) and PEPCK (B) were conducted, and the results were normalized to β-glucuronidase mRNA expression levels. Data represent means ± SEM of data from three independent experiments, and the values for the control cells were arbitrarily expressed as 1.0. *, $P < 0.01$ compared with the control. (C) At 3 days posttransfection, the expression levels of each of the HCV proteins were examined by immunoblot analysis using antibodies against c-Myc, core, NS4A, and GAPDH. The amounts of GAPDH served as an internal control to verify equal amounts of sample loading. (D) NS5A and NS4A enhance PEPCK promoter activity. NS5A and NS4A expression plasmids were each cotransfected with rPEPCK-P5(−1263)-pGL3basic or rPEPCK-P4(−998)-pGL3basic in Huh-7.5 cells. At 48 h after transfection, the PEPCK promoter activities were measured by using a luciferase reporter assay. Data represent means ± SEM of data from three independent experiments, and the values for the control cells were arbitrarily expressed as 1.0. *, $P < 0.05$ compared with the control.

phosphorylation, the nuclear accumulation of FoxO1, and the enhancement of glucose production in HCV-infected cells.

HCV NS5A is involved in the enhancement of glucose production. To examine which HCV protein(s) is involved in the enhancement of gluconeogenesis, expression constructs of each of the HCV viral proteins were transfected into Huh-7.5 cells, and the gene expression levels of PEPCK and G6Pase were examined by real-time quantitative RT-PCR analysis. We observed that NS5A significantly promoted G6Pase gene expression (Fig. 7A). Moreover, both the NS5A and NS4A proteins significantly enhanced PEPCK gene expression at 3 and 5 days posttransfection, respectively (Fig. 7B). The expression of each of the HCV proteins except NS2 was verified by immunoblot analysis (Fig. 7C). NS2 was reported previously to be unstable and rapidly degraded by the proteasome (22).

Next, we performed a luciferase reporter assay to examine

the possible effects of NS5A and NS4A on PEPCK promoter activities. The construct rPEPCK-P5(−1263)-pGL3basic carries 1,263 bp of the PEPCK 5′-flanking region (−1263 PEPCK) and is used to monitor PEPCK promoter activity. The results demonstrated that the levels of PEPCK promoter activities were significantly higher in both NS5A- and NS4A-expressing cells than in the control cells (Fig. 7D). Interestingly, when the region of the PEPCK promoter from positions −1263 to −998 was deleted, the activation of PEPCK promoter activity in cells expressing NS5A and NS4A was abolished. These results confirmed that NS5A and NS4A activate the PEPCK promoter, leading to an increase in PEPCK mRNA expression levels. Database searches of the deleted sequence did not reveal any potential binding sequences for transcription factors (data not shown).

Recently reported data suggest that ROS production is induced in NS5A-expressing cells (17) or in hepatocytes of NS5A transgenic mice (68). We therefore sough to determine whether NS5A contributes to increased hepatic gluconeogenesis through the induction of ROS production. The NS5A expression plasmid was transfected into Huh-7.5 cells, and ROS production was assessed by MitoSOX at 3 days posttransfection. As shown in Fig. 8A and B, approximately 30% of NS5A-expressing cells displayed a much stronger signal than that observed for vector-transfected control cells.

We then examined whether NS5A mediated JNK/c-Jun activation and FoxO1 phosphorylation inhibition. The results obtained revealed that both the phosphorylation level at Ser63 and the total expression level of c-Jun were upregulated in NS5A-expressing cells compared to the control cells transfected with the vector plasmid or cells expressing the other HCV proteins (Fig. 8C and D, top two panels). Concomitantly, FoxO1 phosphorylation at Ser319 was clearly suppressed in NS5A- and NS4A-expressing cells compared to the control cells (Fig. 8C, compare lanes 6, 5, and 1, respectively, in the third panel). NS4A, a small protein of ca. 7 kDa, forms a stable complex with NS3 to function as a cofactor for NS3 serine protease and RNA helicase activities (51). We previously reported that NS4A caused mitochondrial damage when expressed alone but not when coexpressed with NS3 (47). We therefore speculated that the otherwise observed decrease in FoxO1 phosphorylation levels in NS4A-expressing cells might be canceled when NS4A is coexpressed with NS3. To verify this notion, we tested FoxO1 phosphorylation in cells coexpressing NS3 and NS4A. As had been expected, FoxO1 phosphorylation levels did not differ between NS3/4A-coexpressing cells and vector-transfected control cells (Fig. 8C, compare lanes 4 and 1, respectively).

Notably, we observed that the HCV core protein did not alter the phosphorylation status of c-Jun and FoxO1 (Fig. 8C, compare lanes 1 and 2), with the result being consistent with what was observed for gene expression levels of PEPCK and G6Pase in HCV core-expressing cells (Fig. 7A and B). These results imply that core is not primarily involved in HCV-induced increased gluconeogenesis under our experimental conditions. Similarly, other HCV nonstructural proteins, such as NS4B and NS5B, did not significantly influence the phosphorylation status of c-Jun and FoxO1 (Fig. 8D).

In order to further verify the effect of NS5A on the nuclear accumulation of FoxO1, we examined the subcellular localization of FoxO1 in NS5A-expressing cells by indirect immunofluorescence staining. As shown in Fig. 8E and F, the nuclear accumulation of FoxO1 was clearly observed for approximately 25% of NS5A-expressing cells but not the vector-transfected control. These results suggest that NS5A activates the JNK/c-Jun signaling pathway via increased ROS production, which results in the decreased phosphorylation and nuclear accumulation of FoxO1.

Finally, we examined the effects of NS5A and NS4A on glucose production. As shown in Fig. 9, the amounts of glucose were significantly increased in culture supernatants of NS5A- and NS4A-expressing cells, compared with the amounts of glucose in control cells, at 5 days posttransfection. Again, it is reasonable to assume that the observed increase in glucose production in NS4A-expressing cells might be canceled when NS4A is coexpressed with NS3.

These results collectively suggest that NS5A plays a role, at least to some extent, in the HCV-induced enhancement of hepatic gluconeogenesis.

DISCUSSION

Hepatocytes play an important role in maintaining plasma glucose homeostasis by adjusting the balance between hepatic glucose production and utilization via the gluconeogenic and glycolytic pathways, respectively. We previously reported that HCV suppresses cellular glucose uptake by downregulating the surface expression of the glucose transporters GLUT1 and GLUT2 (37). In this study, we have demonstrated that HCV promotes FoxO1-mediated hepatic gluconeogenesis, as evidenced by the increased accumulation of FoxO1 in the nucleus via the reduction of its phosphorylation status (Fig. 3 and 6A and B), which leads to increased PEPCK and G6Pase gene expression levels (Fig. 1A and B) and the subsequent upregulation of G6P and glucose production (Fig. 2). Moreover, our results indicate that HCV-induced ROS production causes JNK activation, which results in the decreased phosphorylation and nuclear accumulation of FoxO1, leading eventually to increased glucose production (Fig. 4 to 6). Our results thus suggest that FoxO1 is a prime transcription factor in the HCV-mediated progression of hepatic gluconeogenesis through an ROS/JNK-dependent mechanism, as summarized in the schema in Fig. 10. Our results also suggest that HCV NS5A plays a role in enhanced hepatic gluconeogenesis by promoting ROS production and JNK activation (Fig. 7 to 9). In line with our observations, the NS5A-mediated induction of ROS production (68) and JNK activation (49) was reported previously by other investigators.

Increasing evidence suggests that mitochondrial dysfunction is causative of insulin resistance and type 2 diabetes. Mitochondrial dysfunction causes the upregulation of PEPCK and G6Pase, leading to increased gluconeogenesis and insulin resistance (42, 46). We previously reported that HCV causes mitochondrial damage and mitochondrion-mediated apoptosis (14, 47). Our current data further support the concept that altered mitochondrial function plays a role in the development of increased glucose production in hepatocytes.

We and other groups have reported that HCV infection increases the production of mitochondrial ROS, which plays an important role in the development and progression of inflam-

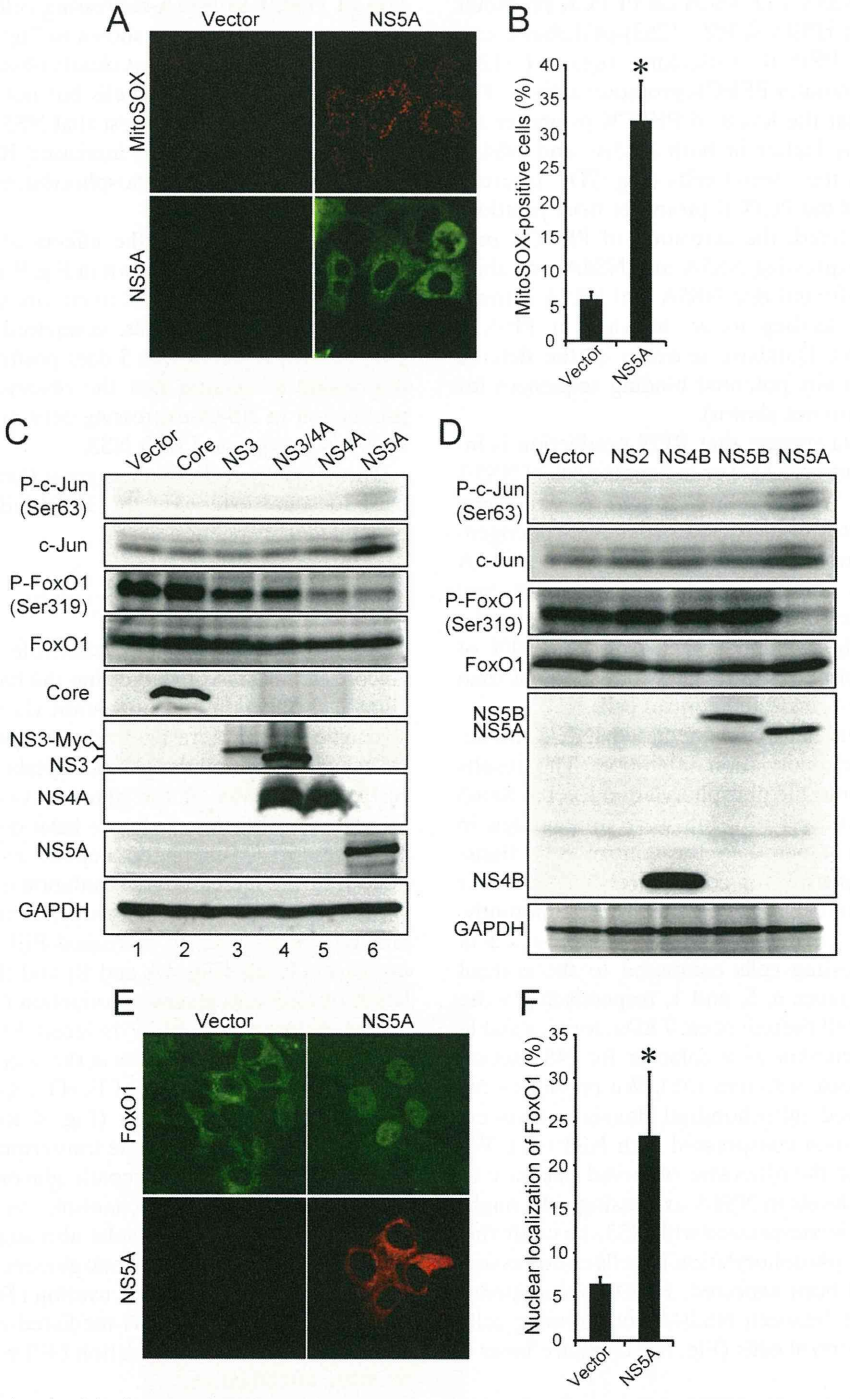

FIG. 8. HCV NS5A is involved in increased ROS production, JNK activation, FoxO1 phosphorylation suppression, and FoxO1 nuclear accumulation. (A) NS5A promotes ROS production. Huh-7.5 cells transfected with an NS5A expression plasmid or the empty control (vector) were incubated with MitoSOX (top) at 3 days posttransfection and then stained for NS5A by using anti-NS5A mouse monoclonal antibody, followed by FITC-conjugated goat anti-mouse IgG (bottom). (B) Quantification of MitoSOX-stained cells. The percentages of cells stained with MitoSOX were determined for NS5A-expressing cells and control cells. Data represent means ± SEM of data from two independent experiments. *, $P < 0.01$. (C and D) HCV NS5A activates c-Jun phosphorylation and suppresses FoxO1 phosphorylation. Huh-7.5 cells transfected with the indicated HCV viral protein expression plasmids were harvested at 3 days posttransfection, and the whole-cell lysates were subjected to immunoblot analysis using antibodies against phospho-c-Jun (Ser63), c-Jun, phospho-FoxO1 (Ser319), FoxO1, GAPDH, core, NS3, NS4A, and NS5A (C) or c-Myc (D). The amounts of GAPDH were measured as an internal control to verify equal amounts of sample loading. (E) NS5A facilitates FoxO1 nuclear accumulation. Huh-7.5 cells transfected with an NS5A expression plasmid or the empty control (vector) were fixed and permeabilized at 3 days posttransfection. The cells were incubated with an anti-FoxO1 rabbit monoclonal antibody followed by Alexa Fluor 488-conjugated goat anti-rabbit IgG (top) or with anti-NS5A mouse monoclonal antibody followed by Alexa Fluor 594-conjugated goat anti-mouse IgG (bottom). (F) The percentages of cells with a nuclear localization of FoxO1 were determined for NS5A-expressing cells and control cells. Data represent means ± SEM of data from two independent experiments. *, $P < 0.01$.

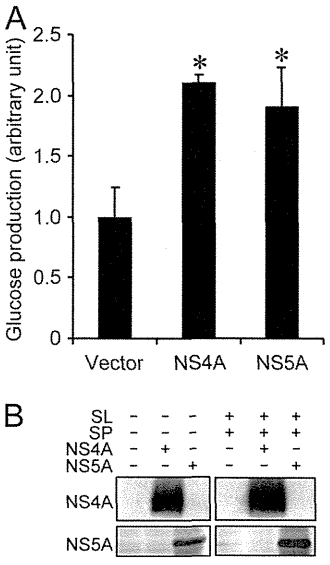

FIG. 9. HCV NS5A and NS4A enhance glucose production. (A) Huh-7.5 cells were transfected with either an NS5A or NS4A expression plasmid. At 5 days posttransfection, extracellular glucose production was measured and normalized to the total cellular protein expression level. Data represent means ± SEM of data from two independent experiments, and the values for the control cells were arbitrarily expressed as 1.0. *, $P < 0.05$ compared with the control. (B) Cellular expression levels of NS4A and NS5A in the absence and presence of sodium lactate (SL) and sodium pyruvate (SP) are shown.

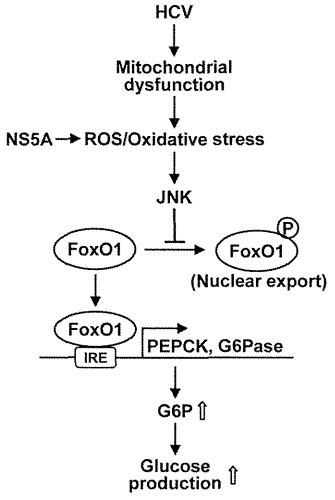

FIG. 10. Schematic representation of the HCV-dysregulated hepatic gluconeogenesis signaling pathway. HCV induces mitochondrial dysfunction (14). This results in increased ROS production and JNK activation, which induces the nuclear accumulation of FoxO1 by reducing its phosphorylation status. Consequently, PEPCK and G6Pase gene expressions are upregulated, leading to an upregulation of G6P and glucose production. NS5A plays a role in HCV-induced gluconeogenesis via the induction of ROS production. IRE, insulin response element.

matory liver disease mediated by HCV (12, 14). Increased mitochondrial ROS generation was also shown previously to be an underlying mediator of multiple forms of insulin resistance, including inflammation- or glucocorticoid-induced insulin resistance (27, 29). Moreover, a significant correlation was observed between oxidative stress and insulin resistance in patients infected with HCV genotype 1 or 2 (44). ROS have also been shown to regulate the activity of the FoxO transcription factor by posttranslational modifications, including phosphorylation (21), deacetylation (8), and ubiquitylation (67).

Although this study showed that JNK induces the nuclear accumulation of FoxO1 by reducing its phosphorylation status under oxidative stress conditions in HCV-infected cells, the precise mechanism(s) of the interplay between JNK and FoxO1 still remains to be addressed. It was reported previously that activated JNK phosphorylates IRS-1 at Ser307, which results in attenuated insulin signal transduction through the inhibition of the tyrosine phosphorylation of IRS-1 (1). Akt is a major downstream signaling protein for insulin/IRS-1 signaling and is activated through its phosphorylation on Thr308 and Ser473, the latter of which is believed to be more crucial (53). Therefore, an impairment of the insulin/IRS-1 signaling pathway should involve the downregulation of Akt phosphorylation. However, our present data showed that Akt phosphorylation on Ser473 was upregulated in HCV-infected cells at 4 and 6 dpi (Fig. 3B), suggesting that an Akt-independent pathway is involved in the JNK-mediated suppression of FoxO1 phosphorylation. Regarding this connection, it should be noted that the 14-3-3 protein, a binding partner for phosphorylated FoxO1 that mediates its nuclear export (72), is phosphorylated by JNK and that the phosphorylated 14-3-3 protein releases its binding partners, which would facilitate the nuclear accumulation of FoxO (63, 65, 70). Further studies are needed to elucidate this issue.

Another trigger that causes excessive JNK activation and insulin resistance is endoplasmic reticulum (ER) stress (28, 48). Several previous studies reported that HCV infection induces ER stress (34, 55). Under our experimental conditions, however, we did not detect significant ER stress in HCV-infected cells (14). It is thus likely that ER stress was not the primary cause of the increased gluconeogenesis in our experimental system using Huh-7.5 cells and the P-47 strain of HCV J6/JFH-1 (9, 14).

Notably, our present data showed that cells harboring the SGR or FGR and HCV-infected cells produced greater amounts of glucose than did the control cells (Fig. 2A); however, the changes in the phosphorylation status of FoxO1 and JNK in SGR- and FGR-harboring cells were not so significant compared to those in virus-infected cells (data not shown). One of the reasons for this difference is that SGR- and FGR-harboring cells were obtained through a longer cultivation in a selection medium for a month or more and that the balance of host gene induction may be somewhat different from that in virus-infected cells. Therefore, it is possible that, in addition to the JNK-FoxO1 pathway, another signaling pathway(s) is involved in the increased gluconeogenesis in SGR- and FGR-harboring cells. Studies on this issue are now under way in our laboratory.

We observed that HCV infection modulated, either positively or negatively, the transcription of the PEPCK, G6Pase, and GK genes at 3 to 5 dpi (Fig. 1). Virus infection, in general, causes dynamically changing induction and the suppression of a wide variety of host genes. For example, expression levels of certain genes, such as interferon genes, increase during an

early phase of virus infection, e.g., at 1 dpi, but return to normal levels within a few days in a cell culture system. On the other hand, the virus-infection-induced expression of other genes, such as the extracellular signal-regulated kinase (ERK) gene, remains for a prolonged period of time (data not shown). Also, some of the gene products induced in the acute phase may suppress the expression of other genes. Under these balanced conditions, it is quite possible that certain genes are induced only at a later time, e.g., 3 to 5 dpi, but not immediately after virus infection.

It was reported previously that HCV core protein-expressing transgenic mice exhibit marked insulin resistance by inhibiting IRS-1 tyrosine phosphorylation and Akt phosphorylation (45, 58). However, our present results showed that HCV NS5A, but not the core protein, was associated with increased gluconeogenesis. Moreover, it was recently reported that HCV infection significantly inhibited cellular glucose levels at 10 dpi (69), which is quite the opposite of what we observed in the present study. These results collectively suggest the possibility that multiple pathways are involved in glucose metabolism in HCV-infected cells. Also, the possible effect(s) of the dysregulation of hepatic gluconeogenesis on the HCV life cycle needs to be clarified.

In conclusion, our present results collectively suggest that HCV promotes hepatic gluconeogenesis, resulting in increased glucose production in hepatocytes via an NS5A-mediated, FoxO1-dependent pathway.

ACKNOWLEDGMENTS

We are grateful to C. M. Rice (Rockefeller University, New York, NY) for providing Huh-7.5 cells and pFL-J6/JFH1, R. Bartenschlager (University of Heidelberg, Heidelberg, Germany) for providing an HCV subgenomic RNA replicon (pFK5B/2884Gly), and N. Kato (Okayama University, Okayama, Japan) for providing an HCV full-length RNA replicon (pON/C-5B). We also thank T. Adachi (Kyoto Prefectural University of Medicine, Kyoto, Japan), K. Igarashi, K. Kashikura, and A. Suzuki (Keio University, Yamagata, Japan) for their technical assistance.

This work was supported in part by grants-in-aid for research on hepatitis from the Ministry of Health, Labor, and Welfare, Japan, and the Japan Initiative for Global Research Network on Infectious Diseases (J-GRID) program of the Ministry of Education, Culture, Sports, Science, and Technology, Japan. This study was also carried out as part of the Global Center of Excellence program of the Kobe University Graduate School of Medicine and the Science and Technology Research Partnership for Sustainable Development (SATREPS) program of the Japan Science and Technology Agency (JST) and the Japan International Cooperation Agency (JICA).

REFERENCES

1. **Aguirre, V., T. Uchida, L. Yenush, R. Davis, and M. F. White.** 2000. The c-Jun NH(2)-terminal kinase promotes insulin resistance during association with insulin receptor substrate-1 and phosphorylation of Ser(307). J. Biol. Chem. **275:**9047–9054.
2. **Alaei, M., and F. Negro.** 2008. Hepatitis C virus and glucose and lipid metabolism. Diabetes Metab. **34:**692–700.
3. **Aytug, S., D. Reich, L. E. Sapiro, D. Bernstein, and N. Begum.** 2003. Impaired IRS-1/PI3-kinase signaling in patients with HCV: a mechanism for increased prevalence of type 2 diabetes. Hepatology **38:**1384–1392.
4. **Banerjee, A., K. Meyer, B. Mazumdar, R. B. Ray, and R. Ray.** 2010. Hepatitis C virus differentially modulates activation of forkhead transcription factors and insulin-induced metabolic gene expression. J. Virol. **84:**5936–5946.
5. **Baron, A. D., L. Schaeffer, P. Shragg, and O. G. Kolterman.** 1987. Role of hyperglucagonemia in maintenance of increased rates of hepatic glucose output in type II diabetics. Diabetes **36:**274–283.
6. **Bennett, B. L., et al.** 2001. SP600125, an anthrapyrazolone inhibitor of Jun N-terminal kinase. Proc. Natl. Acad. Sci. U. S. A. **98:**13681–13686.
7. **Blight, K. J., J. A. McKeating, and C. M. Rice.** 2002. Highly permissive cell lines for subgenomic and genomic hepatitis C virus RNA replication. J. Virol. **76:**13001–13014.
8. **Brunet, A., et al.** 2004. Stress-dependent regulation of FOXO transcription factors by the SIRT1 deacetylase. Science **303:**2011–2015.
9. **Bungyoku, Y., et al.** 2009. Efficient production of infectious hepatitis C virus with adaptive mutations in cultured hepatoma cells. J. Gen. Virol. **90:**1681–1691.
10. **Burdette, D., M. Olivarez, and G. Waris.** 2010. Activation of transcription factor Nrf2 by hepatitis C virus induces the cell-survival pathway. J. Gen. Virol. **91:**681–690.
11. **Caronia, S., et al.** 1999. Further evidence for an association between non-insulin-dependent diabetes mellitus and chronic hepatitis C virus infection. Hepatology **30:**1059–1063.
12. **Choi, J., and J. H. Ou.** 2006. Mechanisms of liver injury. III. Oxidative stress in the pathogenesis of hepatitis C virus. Am. J. Physiol. Gastrointest. Liver Physiol. **290:**G847–G851.
13. **Clore, J. N., J. Stillman, and H. Sugerman.** 2000. Glucose-6-phosphatase flux in vitro is increased in type 2 diabetes. Diabetes **49:**969–974.
14. **Deng, L., et al.** 2008. Hepatitis C virus infection induces apoptosis through a Bax-triggered, mitochondrion-mediated, caspase 3-dependent pathway. J. Virol. **82:**10375–10385.
15. **Deng, L., et al.** 2006. NS3 protein of hepatitis C virus associates with the tumour suppressor p53 and inhibits its function in an NS3 sequence-dependent manner. J. Gen. Virol. **87:**1703–1713.
16. **Diamond, D. L., et al.** 2010. Temporal proteome and lipidome profiles reveal hepatitis C virus-associated reprogramming of hepatocellular metabolism and bioenergetics. PLoS Pathog. **6:**e1000719.
17. **Dionisio, N., et al.** 2009. Hepatitis C virus NS5A and core proteins induce oxidative stress-mediated calcium signalling alterations in hepatocytes. J. Hepatol. **50:**872–882.
18. **Doi, H., C. Apichartpiyakul, K. I. Ohba, M. Mizokami, and H. Hotta.** 1996. Hepatitis C virus (HCV) subtype prevalence in Chiang Mai, Thailand, and identification of novel subtypes of HCV major type 6. J. Clin. Microbiol. **34:**569–574.
19. **Dunning, B. E., and J. E. Gerich.** 2007. The role of alpha-cell dysregulation in fasting and postprandial hyperglycemia in type 2 diabetes and therapeutic implications. Endocr. Rev. **28:**253–283.
20. **Eslam, M., M. A. Khattab, and S. A. Harrison.** 2011. Insulin resistance and hepatitis C: an evolving story. Gut **60:**1139–1151.
21. **Essers, M. A., et al.** 2004. FOXO transcription factor activation by oxidative stress mediated by the small GTPase Ral and JNK. EMBO J. **23:**4802–4812.
22. **Franck, N., J. Le Seyec, C. Guguen-Guillouzo, and L. Erdtmann.** 2005. Hepatitis C virus NS2 protein is phosphorylated by the protein kinase CK2 and targeted for degradation to the proteasome. J. Virol. **79:**2700–2708.
23. **Galossi, A., R. Guarisco, L. Bellis, and C. Puoti.** 2007. Extrahepatic manifestations of chronic HCV infection. J. Gastrointestin. Liver Dis. **16:**65–73.
24. **Gottwein, J. M., et al.** 2009. Development and characterization of hepatitis C virus genotype 1-7 cell culture systems: role of CD81 and scavenger receptor class B type I and effect of antiviral drugs. Hepatology **49:**364–377.
25. **Gross, D. N., A. P. van den Heuvel, and M. J. Birnbaum.** 2008. The role of FoxO in the regulation of metabolism. Oncogene **27:**2320–2336.
26. **Hirota, K., et al.** 2008. A combination of HNF-4 and Foxo1 is required for reciprocal transcriptional regulation of glucokinase and glucose-6-phosphatase genes in response to fasting and feeding. J. Biol. Chem. **283:**32432–32441.
27. **Hoehn, K. L., et al.** 2009. Insulin resistance is a cellular antioxidant defense mechanism. Proc. Natl. Acad. Sci. U. S. A. **106:**17787–17792.
28. **Hotamisligil, G. S.** 2005. Role of endoplasmic reticulum stress and c-Jun NH2-terminal kinase pathways in inflammation and origin of obesity and diabetes. Diabetes **54**(Suppl. 2)**:**S73–S78.
29. **Houstis, N., E. D. Rosen, and E. S. Lander.** 2006. Reactive oxygen species have a causal role in multiple forms of insulin resistance. Nature **440:**944–948.
30. **Huang, H., and D. J. Tindall.** 2007. Dynamic FoxO transcription factors. J. Cell Sci. **120:**2479–2487.
31. **Ikeda, M., et al.** 2005. Efficient replication of a full-length hepatitis C virus genome, strain O, in cell culture, and development of a luciferase reporter system. Biochem. Biophys. Res. Commun. **329:**1350–1359.
32. **Inubushi, S., et al.** 2008. Hepatitis C virus NS5A protein interacts with and negatively regulates the non-receptor protein tyrosine kinase Syk. J. Gen. Virol. **89:**1231–1242.
33. **Iynedjian, P. B., et al.** 1989. Differential expression and regulation of the glucokinase gene in liver and islets of Langerhans. Proc. Natl. Acad. Sci. U. S. A. **86:**7838–7842.
34. **Joyce, M. A., et al.** 2009. HCV induces oxidative and ER stress, and sensitizes infected cells to apoptosis in SCID/Alb-uPA mice. PLoS Pathog. **5:**e1000291.
35. **Kamata, H., et al.** 2005. Reactive oxygen species promote TNFalpha-induced death and sustained JNK activation by inhibiting MAP kinase phosphatases. Cell **120:**649–661.
36. **Karpac, J., and H. Jasper.** 2009. Insulin and JNK: optimizing metabolic homeostasis and lifespan. Trends Endocrinol. Metab. **20:**100–106.
37. **Kasai, D., et al.** 2009. HCV replication suppresses cellular glucose uptake

through down-regulation of cell surface expression of glucose transporters. J. Hepatol. **50:**883–894.
38. **Kops, G. J., and B. M. Burgering.** 1999. Forkhead transcription factors: new insights into protein kinase B (c-akt) signaling. J. Mol. Med. **77:**656–665.
39. **Lindenbach, B. D., et al.** 2005. Complete replication of hepatitis C virus in cell culture. Science **309:**623–626.
40. **Lindenbach, B. D., and C. M. Rice.** 2005. Unravelling hepatitis C virus replication from genome to function. Nature **436:**933–938.
41. **Lohmann, V., F. Korner, A. Dobierzewska, and R. Bartenschlager.** 2001. Mutations in hepatitis C virus RNAs conferring cell culture adaptation. J. Virol. **75:**1437–1449.
42. **Lowell, B. B., and G. I. Shulman.** 2005. Mitochondrial dysfunction and type 2 diabetes. Science **307:**384–387.
43. **Mehta, S. H., et al.** 2000. Prevalence of type 2 diabetes mellitus among persons with hepatitis C virus infection in the United States. Ann. Intern. Med. **133:**592–599.
44. **Mitsuyoshi, H., et al.** 2008. Evidence of oxidative stress as a cofactor in the development of insulin resistance in patients with chronic hepatitis C. Hepatol. Res. **38:**348–353.
45. **Miyamoto, H., et al.** 2007. Involvement of the PA28gamma-dependent pathway in insulin resistance induced by hepatitis C virus core protein. J. Virol. **81:**1727–1735.
46. **Morino, K., K. F. Petersen, and G. I. Shulman.** 2006. Molecular mechanisms of insulin resistance in humans and their potential links with mitochondrial dysfunction. Diabetes **55**(Suppl. 2):S9–S15.
47. **Nomura-Takigawa, Y., et al.** 2006. Non-structural protein 4A of hepatitis C virus accumulates on mitochondria and renders the cells prone to undergoing mitochondria-mediated apoptosis. J. Gen. Virol. **87:**1935–1945.
48. **Ozcan, U., et al.** 2004. Endoplasmic reticulum stress links obesity, insulin action, and type 2 diabetes. Science **306:**457–461.
49. **Park, K. J., et al.** 2003. Hepatitis C virus NS5A protein modulates c-Jun N-terminal kinase through interaction with tumor necrosis factor receptor-associated factor 2. J. Biol. Chem. **278:**30711–30718.
50. **Puigserver, P., et al.** 2003. Insulin-regulated hepatic gluconeogenesis through FOXO1-PGC-1alpha interaction. Nature **423:**550–555.
51. **Reed, K. E., and C. M. Rice.** 2000. Overview of hepatitis C virus genome structure, polyprotein processing, and protein properties. Curr. Top. Microbiol. Immunol. **242:**55–84.
52. **Rozance, P. J., et al.** 2008. Chronic late-gestation hypoglycemia upregulates hepatic PEPCK associated with increased PGC1alpha mRNA and phosphorylated CREB in fetal sheep. Am. J. Physiol. Endocrinol. Metab. **294:** E365–E370.
53. **Sale, E. M., and G. J. Sale.** 2008. Protein kinase B: signalling roles and therapeutic targeting. Cell. Mol. Life Sci. **65:**113–127.
54. **Schmoll, D., et al.** 2000. Regulation of glucose-6-phosphatase gene expression by protein kinase Balpha and the forkhead transcription factor FKHR. Evidence for insulin response unit-dependent and -independent effects of insulin on promoter activity. J. Biol. Chem. **275:**36324–36333.
55. **Sekine-Osajima, Y., et al.** 2008. Development of plaque assays for hepatitis C virus-JFH1 strain and isolation of mutants with enhanced cytopathogenicity and replication capacity. Virology **371:**71–85.
56. **Seo, H. Y., et al.** 2010. Endoplasmic reticulum stress-induced activation of activating transcription factor 6 decreases cAMP-stimulated hepatic gluconeogenesis via inhibition of CREB. Endocrinology **151:**561–568.
57. **Shepard, C. W., L. Finelli, and M. J. Alter.** 2005. Global epidemiology of hepatitis C virus infection. Lancet Infect. Dis. **5:**558–567.
58. **Shintani, Y., et al.** 2004. Hepatitis C virus infection and diabetes: direct involvement of the virus in the development of insulin resistance. Gastroenterology **126:**840–848.
59. **Simmonds, P., et al.** 2005. Consensus proposals for a unified system of nomenclature of hepatitis C virus genotypes. Hepatology **42:**962–973.
60. **Soga, T., et al.** 2006. Differential metabolomics reveals ophthalmic acid as an oxidative stress biomarker indicating hepatic glutathione consumption. J. Biol. Chem. **281:**16768–16776.
61. **Soga, T., et al.** 2009. Metabolomic profiling of anionic metabolites by capillary electrophoresis mass spectrometry. Anal. Chem. **81:**6165–6174.
62. **Streeper, R. S., et al.** 1997. A multicomponent insulin response sequence mediates a strong repression of mouse glucose-6-phosphatase gene transcription by insulin. J. Biol. Chem. **272:**11698–11701.
63. **Sunayama, J., F. Tsuruta, N. Masuyama, and Y. Gotoh.** 2005. JNK antagonizes Akt-mediated survival signals by phosphorylating 14-3-3. J. Cell Biol. **170:**295–304.
64. **Takashima, M., et al.** 2010. Role of KLF15 in regulation of hepatic gluconeogenesis and metformin action. Diabetes **59:**1608–1615.
65. **Tsuruta, F., et al.** 2004. JNK promotes Bax translocation to mitochondria through phosphorylation of 14-3-3 proteins. EMBO J. **23:**1889–1899.
66. **van der Horst, A., and B. M. Burgering.** 2007. Stressing the role of FoxO proteins in lifespan and disease. Nat. Rev. Mol. Cell Biol. **8:**440–450.
67. **van der Horst, A., et al.** 2006. FOXO4 transcriptional activity is regulated by monoubiquitination and USP7/HAUSP. Nat. Cell Biol. **8:**1064–1073.
68. **Wang, A. G., et al.** 2009. Non-structural 5A protein of hepatitis C virus induces a range of liver pathology in transgenic mice. J. Pathol. **219:**253–262.
69. **Woodhouse, S. D., et al.** 2010. Transcriptome sequencing, microarray, and proteomic analyses reveal cellular and metabolic impact of hepatitis C virus infection in vitro. Hepatology **52:**443–453.
70. **Yoshida, K., T. Yamaguchi, T. Natsume, D. Kufe, and Y. Miki.** 2005. JNK phosphorylation of 14-3-3 proteins regulates nuclear targeting of c-Abl in the apoptotic response to DNA damage. Nat. Cell Biol. **7:**278–285.
71. **Zhang, S., J. Liu, G. MacGibbon, M. Dragunow, and G. J. Cooper.** 2002. Increased expression and activation of c-Jun contributes to human amylin-induced apoptosis in pancreatic islet beta-cells. J. Mol. Biol. **324:**271–285.
72. **Zhao, X., et al.** 2004. Multiple elements regulate nuclear/cytoplasmic shuttling of FOXO1: characterization of phosphorylation- and 14-3-3-dependent and -independent mechanisms. Biochem. J. **378:**839–849.

Nephro-Urol Mon. 2011;3(3):164-171
Nephro-Urology Monthly
Journal home page: www.NUmonthly.com

Use of serum and urine metabolome analysis for the detection of metabolic changes in patients with stage 1-2 chronic kidney disease

Kaori Hayashi [1], Hiroyuki Sasamura [1*], Takako Hishiki [2], Makoto Suematsu [2], Satsuki Ikeda [3], Tomoyoshi Soga [3], Hiroshi Itoh [1]

[1] Department of Internal Medicine, School of Medicine, Keio University, Tokyo, Japan
[2] Department of Biochemistry, School of Medicine, Keio University, Tokyo, Japan
[3] Institute for Advanced Biosciences, Keio University, Yamagata, Japan

ARTICLE INFO

Article Type:
Original Article

Article history:
Received: 19 Oct 2010
Revised: 1 Nov 2010
Accepted: 20 Nov 2010

Keywords:
Chronic kidney failure
Metabolomics
Mass spectrometry

ABSTRACT

Background: Chronic kidney disease (CKD) is a major health problem throughout the world, and understanding the pathological condition of CKD has become increasingly important. The recent development of advanced metabolomic assay techniques now allows the human metabolic condition to be evaluated sensitively and comprehensively.
Objectives: The aim of this study was to use metabolomic analysis to perform a preliminary survey of metabolic changes occurring in patients with stage 1-2 CKD.
Patients and Methods: Serum and urine metabolomic profiles of 15 patients with stage 1-2 CKD were analyzed using our previously reported capillary electrophoresis time-of-flight mass spectrometry (CE-TOFMS) systems, and compared to 7 healthy volunteers.
Results: The CE-TOFMS systems in three different modes for cation, anion, and nucleotide analyses detected multiple metabolites in serum and urine samples. In cation analysis mode, several increases in nonessential amino acids were identified in patients with stage 1-2 CKD, similar to those reported for end-stage renal disease (ESRD). Free-radical scavengers carnosine and hypotaurine were decreased in the urine, whereas serum hypotaurine and taurine were increased, consistent with changes in renal and/or systemic oxidative stress. Moreover, the cardiotoxin hypoxanthine was markedly increased in the serum, whereas serum and urine adenosine and urine guanine were decreased, suggesting changes in purine nucleotide metabolism which could affect cardiovascular prognosis. Changes in other unidentified metabolites were also detected.
Conclusions: These results suggest that multiple changes in the metabolism are already detectable in stage 1-2 CKD using metabolome analysis. Further studies on these metabolic changes may result in new strategies to prevent cardiovascular events and progression to ESRD in patients with CKD.

▸ *Implication for health policy/practice/research/medical education:*
The results of this study suggest that multiple changes in the metabolism are already detectable in stage 1-2 CKD, and these changes may be detected using metabolome analysis.

▸ *Please cite this paper as:*
Hayashi K, Sasamura H, Hishiki T, Suematsu M, Ikeda S, Soga T, et al. Use of serum and urine metabolome analysis for the detection of metabolic changes in patients with stage 1-2 chronic kidney disease. *Nephro-Urol Mon.* 2011;3(3):164-171.

* *Corresponding author at:* Hiroyuki Sasamura, Department of Internal Medicine, School of Medicine, Keio University, 35 Shinanomachi, Shinjuku-ku, 160-8582, Tokyo, Japan. Tel: +81-35363-3796, Fax: +81-33359-2745.
E-mail: sasamura@a8.keio.jp

1. Background

It has been reported that the prevalence of chronic kidney disease (CKD) has increased to over 10% (1), and is now

a major health problem throughout the world. A number of co-morbidities including cardiovascular diseases are associated with CKD and prognosis is poor, with many patients experiencing disease progression (2). CKD is not only a strong risk factor for cardiovascular diseases (3, 4), but also the precursor of end stage renal failure (ESRD, also known as CKD stage 5), which needs renal replacement therapy such as dialysis. Previous studies using ion-exchange chromatography or HPLC have identified several changes in amino acid metabolism in patients with ESRD (5-8), but a survey of metabolomic changes has not been reported. Metabolomics is a discipline dedicated to the global study of metabolites, their dynamics, composition, interactions, and responses to interventions or to changes in their environment (9). The recent developments of advanced metabolomic assay techniques now allow the human metabolic condition to be evaluated sensitively and comprehensively. Metabolomics has already been reported to be effective for the discovery of biomarkers for disease diagnosis, such as cancer (10, 11) and cardiovascular diseases (12), but its effectiveness for the assessment of renal physiology and kidney disease is still uncertain. Metabolomics may be a useful tool for analyzing the condition of CKD, because CKD is recognized to be a disease affecting multiple biochemical pathways, and thus may cause multiple changes in systemic metabolism. Moreover, CKD is a strong risk factor for cardiovascular disease, which is highly correlated with metabolic changes. Finally, blood and urine examinations are non-invasive procedures, and due to the fact that they identify changes in both systemic and renal metabolism, may be particularly useful for the non-invasive assessment of patients with CKD.

2. Objectives

Because of the potential importance of understanding metabolic changes in patients with CKD, the aim of this study was to examine the serum and urine metabolites of patients with stage 1-2 CKD, using our recently developed CE-TOFMS system (13), and to compare the results to healthy volunteers, in order to see if metabolic changes can be detected at an early stage in CKD.

3. Materials and Methods

3.1. Patient recruitment and sample collection

This study followed the ethical standards of the Helsinki Declaration and was approved by the Ethics Committee of Keio University. Informed consent was obtained from each participant. A total of fifteen patients with stage 1-2 CKD who were admitted to Keio University Hospital, Tokyo, Japan from January 2008 to March 2009 for kidney biopsy were enrolled in this study. Seven healthy volunteers (5 male and 2 female, with no medical problems including urine abnormalities) participated in this study as controls. CKD was defined according to the criteria of the KDIGO group based on the K/DOQI clinical practice guidelines for CKD (3). In accordance with these criteria, stage 1 CKD was defined as CKD with normal or increased GFR (≥ 90 mL/min/1.73 m 2), and stage 2 CKD was defined as CKD with a mild decrease in GFR (60-89 mL/min/1.73 m

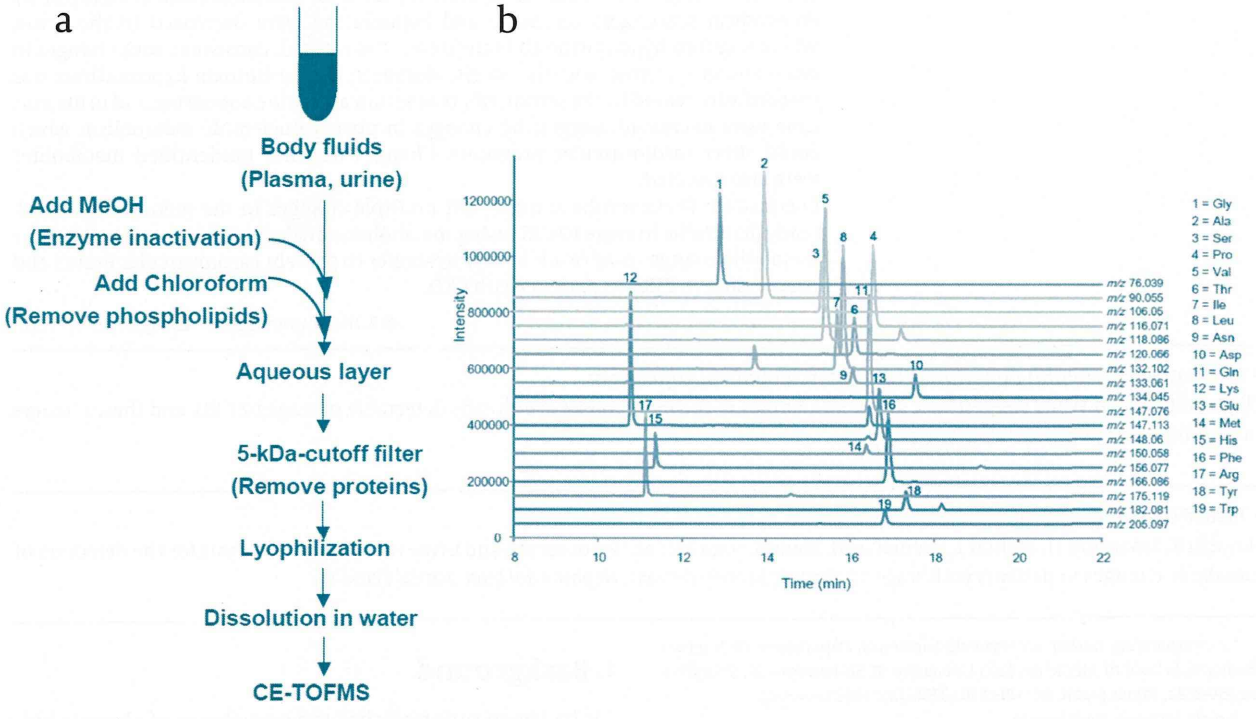

Figure 1. (a) Schematic representation of metabolite extraction method prior to CE-TOFMS analysis. (b) Representative electropherogram of CE-TOFMS.

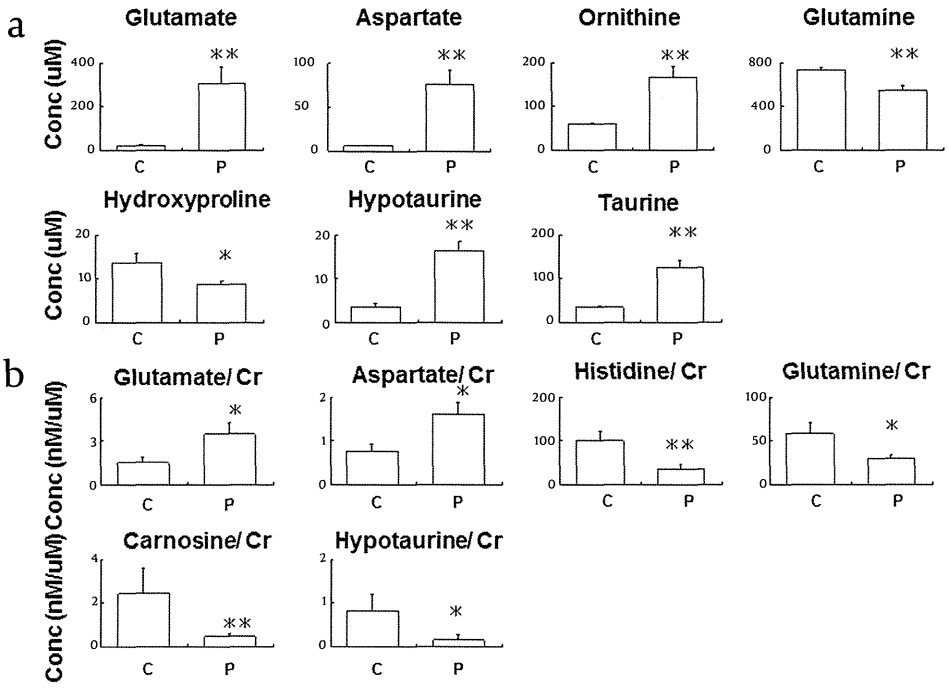

Figure 2. Changes in amino acid metabolites in (a) serum and (b) urine of patients with stage 1-2 CKD. C: Control, P: CKD patients. *, **: $p < 0.05$, $p < 0.01$ vs. controls.

2) (14). Because these patients were candidates for renal biopsy, the presence of proteinuria (≥ 0.5 g/g creatinine) had been checked on at least 3 separate occasions during a period of over 3 months. Moreover, the kidney biopsies were checked in all the patients to confirm that there were no false positive or false negatives in the diagnosis of CKD. Blood and urine samples for metabolomic studies were obtained after an overnight fast. The protocol for urine collection was to void the bladder at bedtime, then to obtain a mid-stream sample from the first morning sample. Samples were then centrifuged without delay at 3000 rpm for 10 min at 4 °C, and the supernatant was stored at - 80 oC until extraction and assay. Values of serum chemistries were obtained using standard hospital laboratory techniques, and GFR was calculated from the age and serum creatinine concentrations.

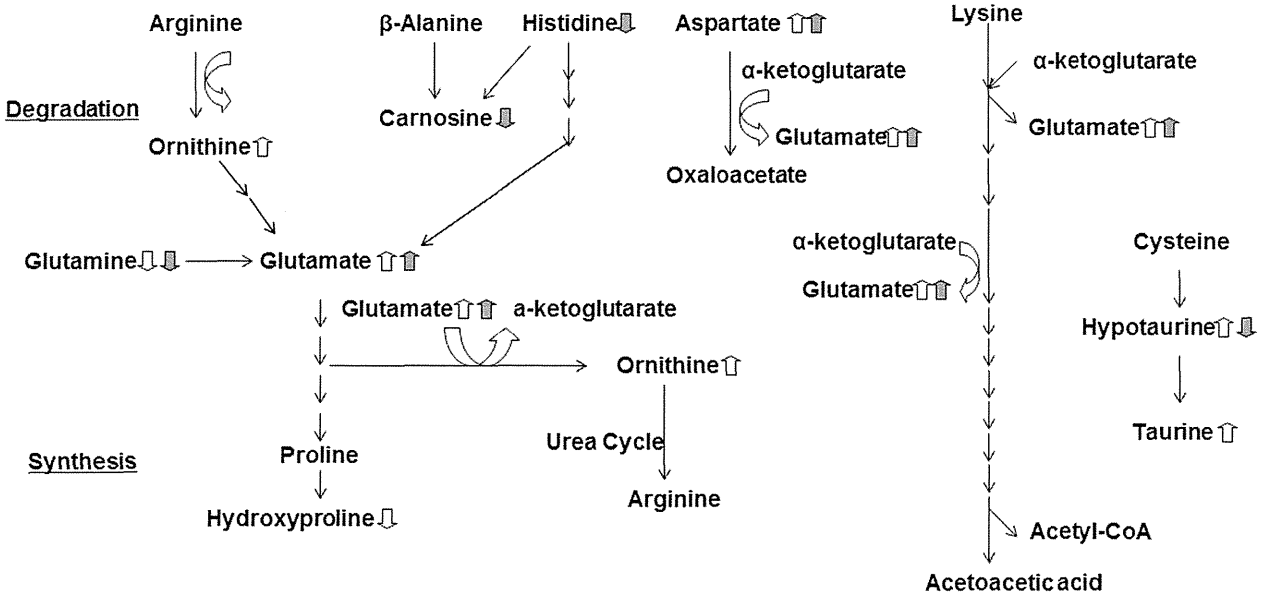

Figure 3. Observed metabolite changes in the serum and urine of patients with stage 1-2 CKD mapped onto the pathways involved in amino acid degradation and synthesis. Open arrows represent significant increases or decreases in serum samples, and closed arrows represent significant changes in urine samples.

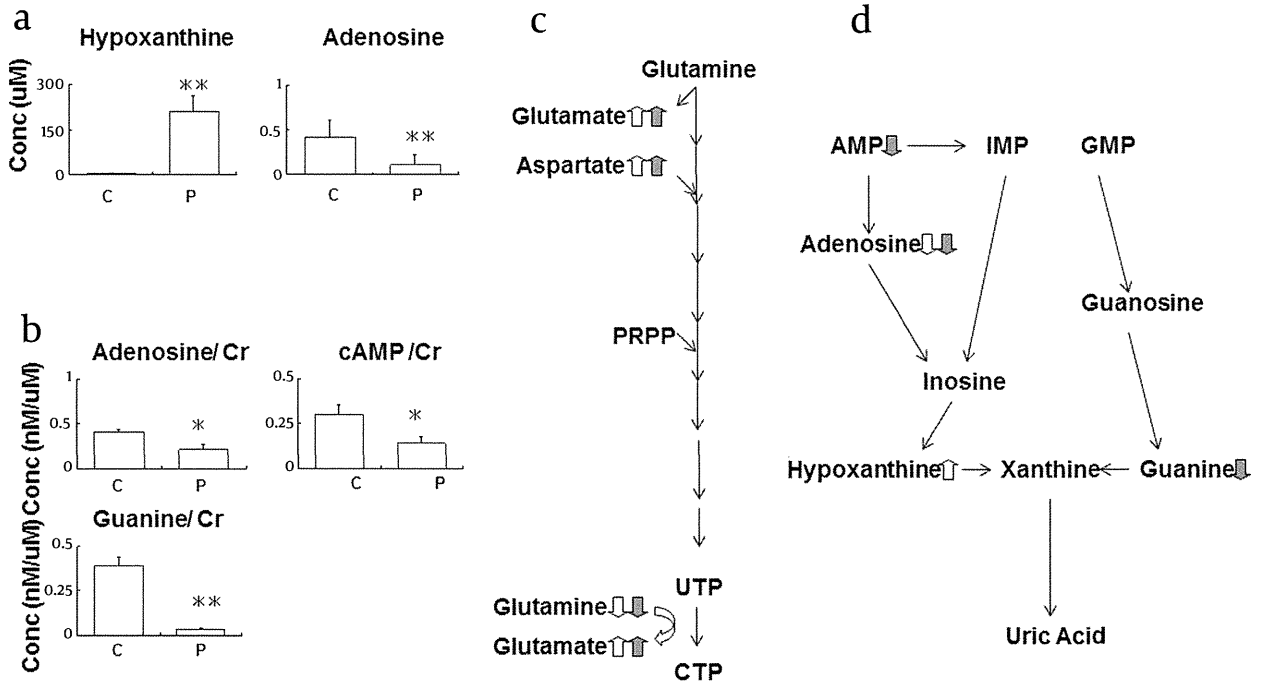

Figure 4. Changes in nucleic acid metabolites in (a) serum and (b) urine of patients with stage 1-2 CKD. Observed metabolite changes mapped onto the pathways involved in (c) pyrimidine nucleotide synthesis and (d) purine nucleotide degradation. Open arrows represent significant increases or decreases in serum samples, and closed arrows represent significant changes in urine samples. *, **: $p < 0.05$, $p < 0.01$ vs. controls.

3.2. Metabolites Extraction

Serum or urine samples (100 ul) were added to methanol (900 ul) containing internal standards (20 uM each of methionine sulfone, MES, and D-Camphol-10-sulfonic acid) and mixed to inactive enzymes. After adding deionized water (400 ul) and chloroform (1 ml), the solution was centrifuged at 4600 g for 5 min at 4 °C and the 300 ul upper aqueous layer was filtered through a Millipore 5-kDa cutoff centrifuge filter to remove proteins. The filtrate was lyophilized and dissolved in 50 ul of Milli-Q water containing reference compounds (200 µl each of 3-aminopyrorridine and trimesate) prior to capillary electrophoresis time-of-flight mass spectrometry (CE-TOFMS) analysis. Samples from patients and controls were prepared and quantified simultaneously to avoid inter-assay variations *(Figure 1)*.

3.3. CE-TOFMS Conditions for Cationic Metabolite Analysis

The instrumentation and measurement conditions of CE-TOFMS are described elsewhere (13, 15, 16). Separations were carried out in a fused silica capillary (50 µm inner diameter x 100 cm total length) filled with 1M formate as the electrolyte. Approximately 3 nl of sample solution were injected at 50 mbar for 3 sec, and 30 kV of Voltage was applied. The capillary was maintained at 20 °C, and the sample tray was cooled below 5 oC. Methanol water (50 % v/v) containing 0.1 µM Hexakis (2,2-difluorothoxy) phosphazene was delivered as the sheath liquid at 10 µl/min.

3.4. CE-TOFMS Conditions for Anionic Metabolite Analysis

A cationic polymer-coated COSMO (+) capillary was used as the separation capillary. A 50mM ammonium acetate solution (pH 8.5) was used as electrolyte solution for CE separation. Sample solution (30 nl) was injected at 50 mbar for 30 s and -30 kV of voltage was applied. Ammonium acetate (5 mM) in 50 % methanol-water (v/v) containing 0.1 µM Hexakis (2, 2-difluorothoxy) phosphazene was delivered as the sheath liquid at 10 µl/min.

3.5. CE-TOFMS Conditions for Nucleotide-related Metabolite Analysis

Separations were carried out in a fused silica capillary filled with 50 mM ammonium acetate (pH 7.5). ESI-TOFMS was operated in the negative ion mode, and the capillary voltage was set at 3500 V. A flow rate of heated dry nitrogen gas (heater temperature 300 °C) was maintained at 7 l/min. Other conditions were identical to those used in anionic metabolite analysis.

3.6. Data processing and statistical analysis

Raw data were analyzed with our proprietary software named MasterHands-1.0.6.16 and JDAMP-128, as described previously (13, 15). For each urine sample, the measured metabolite concentrations were normalized using concentration of creatinine to obtain the amount of metabolite contained (nmol) per creatinine level (µmol) of each sample. Statistical comparisons were made by

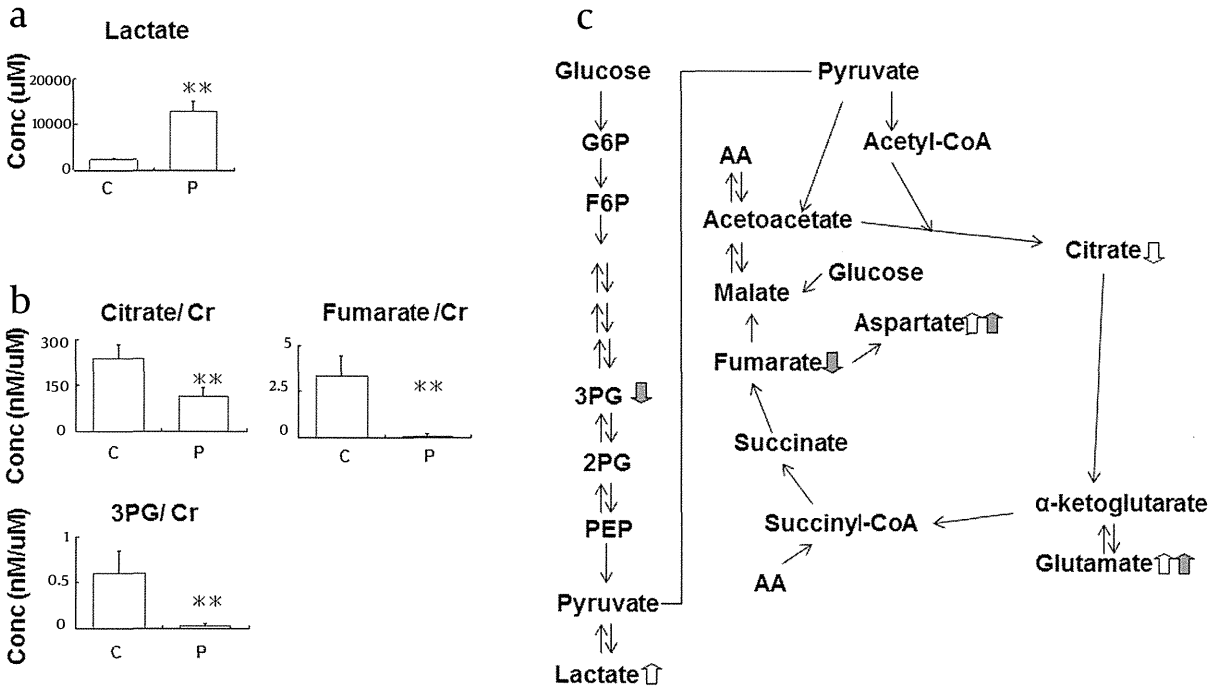

Figure 5. Changes in carbohydrate metabolites in (a) serum and (b) urine of patients with stage 1-2 CKD. (c) Observed metabolite changes mapped onto carbohydrate metabolic pathways. Open arrows represent significant increases or decreases in serum samples, and closed arrows represent significant changes in urine samples. C: Control, P: CKD patients. **: $p < 0.01$ vs. controls.

Mann-Whitney's U-test. P values < 0.05 were considered to be statistically significant.

4. Results

4.1. Baseline characteristics

Serum and urine metabolite profiles were compared between 15 patients with stage 1-2 CKD and 7 healthy volunteers. The baseline characteristics of the patients and controls are shown in *Table 1*. The two groups were similar in age, gender, BMI, and blood pressure. Estimated GFR (eGFR) in patients with stage 1-2 CKD showed a significant decrease (74.84 ± 4.30 ml/min/1.73m2, $p < 0.01$), which was compatible with the definition of stage 1-2 CKD patients, where stage 1 is defined as renal function of 90 ml/min/1.73 m2 or greater, and stage 2 as 60-89 ml/min/1.73 m2 respectively. Blood urea nitrogen and creatinine levels were not significantly different between the two groups. 24-h urinary protein excretion was increased in the patient group, whereas the value in controls was below the detectable threshold.

4.2. Changes in amino acid metabolites in the serum and urine of patients with stage 1-2 CKD

The CE-TOFMS systems in three different modes for cation, anion, and nucleotide analyses detected multiple metabolites, in serum and urine samples. In cation analysis mode, various changes in amino acid metabolites were found in the serum and urine of patients with early stage CKD compared to healthy volunteers *(Figure 2, 3)*. Several nonessential amino acids, in particular glutamate, asparatate, and ornithine were significantly increased in the serum (glutamate: from 22.7 ± 2.7 to 294.7 ± 78.8; aspartate: from 5.7 ± 0.5 to 76.2 ± 16.2; ornithine: from 59.4 ± 3.1 to 167.1 ± 24.4 μM, $p < 0.01$). Similar increases were found in the urine for glutamate and aspartate. In contrast, the essential amino acid histidine was decreased in the urine (from 100.6 ± 24.2 to 36.6 ± 9.1 nM/uM, $p < 0.01$). Both serum and urine glutamine were significantly decreased, suggesting a possible change in the equilibrium for glutamine-glutamate conversion by glutamine synthetase. Hydroxyproline was significantly

Table 1. Clinical characteristics of patients included in the study

Variable	Control (No. = 7)	CKD patients (No. = 15)
Age	30.9 ± 5.0	43.7 ± 4.2
Sex (male/female)	5/2	10/5
Body Mass Index (kg/m2)	20.4 ± 0.6	21.7 ± 0.9
Systolic BP (mmHg)	112 ± 4	121 ± 3
Diastolic BP (mmHg)	73 ± 4	75 ± 3
Blood urea nitrogen (mg/dl)	12.4 ± 1.0	14.3 ± 1.0
Serum creatinine (mg/dl)	0.74 ± 0.05	0.83 ± 0.03
eGFR (ml/min/1.73m2)	101.71 ± 4.88	74.84 ± 4.30 [a]
Serum uric acid (mg/dl)	5.4 ± 0.4	6.1 ± 0.4
Urine protein (g/day)	below threshold	1.35 ± 0.32

[a] $p < 0.01$ vs. controls